Papéis Avulsos de Zoologia
Museu de Zoologia da Universidade de São Paulo

ARTICLE

On two new genera of Trichomycteridae (Teleostei, Siluriformes), with reallocation of some previously described taxa and discussion of phylogenetic relationships

Mario de Pinna[1,4]; Vinicius José Carvalho Reis[1,2,5] & Carlos DoNascimiento[3,6]

[1] Universidade de São Paulo, Museu de Zoologia. São Paulo, SP, Brasil.
[2] Universidade Estadual Paulista "Júlio de Mesquita Filho", Instituto de Biociências, Departamento de Biologia Estrutural e Funcional. Botucatu, SP, Brasil.
[3] Universidad de Antioquia, Facultad de Ciencias Exactas y Naturales, Instituto de Biología, Grupo de Ictiología. Medellín, Antioquía, Colombia.
[4] ORCID: https://orcid.org/0000-0003-1711-4816. E-mail: pinna@ib.usp.br
[5] ORCID: https://orcid.org/0000-0001-7163-9889. E-mail: carvalhvinicius@gmail.com
[6] ORCID: https://orcid.org/0000-0002-8680-7942. E-mail: c.donascimiento@udea.edu.co

Abstract. Two new genera are established for resolving some obvious disparities in current trichomycterid classification. *Salpynx* is described for a monophyletic group of four species from northern shield regions of the Amazon basin, including two new ones described herein plus two others previously described: *S. ephebus,* new species, from Serra da Mocidade in the Rio Branco system, *S. trombetensis,* new species, from the Rio Trombetas drainage, *S. amapaensis* (previously in *Ammoglanis*) from the Rio Jari and surrounding basins, and *S. ix* (previously in *Stenolicmus*) from the Rio Trombetas. Species of *Salpynx* are opaque darkly pigmented fishes with an entirely closed skull roof (*i.e.,* no cranial fontanels) and apomorphically diagnosed by a thick barbular bone posteriorly expanded and bilobed, and a large fenestra on the supratemporal region of the skull, anteriorly to the tunnel for the dorsal limb of the cleithrum. A second new genus, *Hyaloglanis,* is established for a clade of miniaturized species previously placed in *Ammoglanis,* namely, *A. natgeorum, A. nheengatu, A. obliquus,* and *A. pulex. Hyaloglanis* species are extremely miniaturized and highly translucent, with a single large fontanel occupying most of the skull roof and sharing an apomorphic scythe-shaped lacrimal. *Salpynx* and *Hyaloglanis* share various unusual conditions in trichomycterids, such as a reduction of the latero-sensory canal system in the skull, which anteriorly extends maximally to the sphenotic, a palatine articulating directly posteriorly with the skull and via a single articular facet, the posterolateral process of the palatine reduced and deflected laterally, lateral ethmoids mesially arched and abuting against each other only at a small area anteriorly, and a long filamentous first pectoral-fin ray. Although clear morphological evidence exists for the monophyly each of *Salpynx* and *Hyaloglanis,* difficulties remain in determining their precise phylogenetic placement. Such limitations highlight current challenges in the resolution of relationships of part of the Trichomycteridae, especially concerning Glanapteryginae (including *Listrura*), *Potamoglanis,* and Sarcoglanidinae (including *Microcambeva*). It seems certain, however, that neither *Salpynx* nor *Hyaloglanis* are closely related to the type species of either *Ammoglanis* or *Stenolicmus.* At the moment, morphological evidence favors them as each other's sister group and related to Glanapteryginae (*sensu lato*).

Keywords. Glanapteryginae; Rio Branco; Rio Trombetas; Sarcoglanidinae; Systematics; Taxonomy.

INTRODUCTION

The subfamilies Glanapteryginae and Sarcoglanidinae are arguably the most unstable and complex parts of trichomycterid phylogeny. This situation contrasts with that of all other traditional subfamilies of Trichomycteridae (Copionodontinae, Trichogeninae, Trichomycterinae, Tridentinae, Stegophilinae, Vandelliinae), which are nowadays monophyletic on a consensual or nearly consensual basis, both on molecular and morphological evidence (Ochoa *et al.,* 2017, 2020; Reis *et al.,* in press). An expression of that controversy is the recently-proposed subfamily Microcambevinae, which joins one former glanapterygine genus (*Listrura* de Pinna, 1988) with a former sarcoglanidine (*Microcambeva* Costa & Bockmann, 1994) on the basis nearly exclusively of molecular data (Costa *et al.,* 2019a). The situation is further compounded by the genus *Potamoglanis* Henschel *et al.,* 2017, which does not fit properly into any subfamily. From a morphological standpoint, the

Pap. Avulsos Zool., 2025; v.65: e202565027
https://doi.org/10.11606/1807-0205/2025.65.027
https://www.revistas.usp.br/paz
https://www.scielo.br/paz
Edited by: Murilo Nogueira de Lima Pastana
Received: 03/07/2025
Accepted: 18/07/2025
Published: 31/07/2025

ISSN On-Line: 1807-0205
ISSN Printed: 0031-1049
ISNI: 0000-0004-0384-1825
https://zoobank.org/C38896A4-44F3-4E79-B756-0F628AF71FD8

situation is in part the result of the highly aberrant morphologies of some of the taxa included in both Glanapteryginae and Sarcoglanidinae, which are some of the most bizarre-looking catfishes anywhere. Sand-dwelling Amazonian species of *Pygidianops* Myers, 1944 and *Typhlobelus* Myers, 1944 have lost or greatly reduced most of their fins and pigmentation, and superficially resemble protochordates of the amphioxus type (*e.g.,* de Pinna & Kirovsky, 2011). An equally unusual but partly different set of characteristics occurs in eel-like species of *Glanapteryx* Myers, 1927. For a time, the litter-inhabiting species of *Listrura,* from Eastern Brazilian drainages, were considered as a somewhat more generalized glanapterygine, but today there are controversies about their phylogenetic affinities (Ochoa *et al.,* 2020; Costa *et al.,* 2019a; Costa & Katz, 2021; Reis *et al.* in press). Phenotypically, there is clearly a long evolutionary branch separating currently known glanapterygines from remaining trichomycterids. The same applies to Sarcoglanidinae, with the Amazonian *Sarcoglanis* Myers & Weitzman, 1966 and *Malacoglanis* Myers & Weitzman, 1966 being extremely divergent forms, and *Stauroglanis,* de Pinna, 1989, *Stenolicmus,* de Pinna & Starnes, 1990, *Ammoglanis* Costa, 1994, and *Microcambeva* (this one also currently controversial as to subfamilial placement) somewhat less so.

The phylogenetic relationships of glanapterygines have been investigated in some contributions focusing on morphology (Baskin, 1973; de Pinna, 1988, 1989; Costa & Bockmann, 1994; Reis, 2023). However, the hypotheses available, including monophyly of the subfamily, have so far relied on relatively few characters and sparse taxonomic representation. Still, the challenge from competing morphological evidence has been even scantier (Costa & Katz, 2021). Efforts based on sequence data (Ochoa *et al.,* 2020; Costa & Katz, 2021) have yielded surprisingly divergent inferences of relationships, with some glanapterygine taxa grouping with some members of Sarcoglanidinae or placed in a clade sister to subfamilies of the TSVSG clade. Molecular data have yet to be explored to their full potential, mostly because the taxonomic density available is still insufficient due to the rarity of many forms. Recent investigations have also suggested that part of the conflict may be the result of highly divergent evolutionary rates and long-branch attraction (Reis, 2023; Reis *et al.,* in press). The same phenomenon was recently demonstrated to be the source of the controversy regarding Diplomystidae *vs.* Loricarioidei as sister group to all other siluriforms (Rivera-Rivera & Montoya-Burgos, 2018; de Pinna *et al.,* in press).

Herein we report on new species from the northern Shield region of South America which represent a novel combination of morphological features for trichomycterids. In general body shape, the new forms have a generalized aspect not remarkably divergent from that in species of the subfamily Trichomycterinae and some Sarcoglanidinae. Despite that, their internal anatomy is entirely at odds with expectations and instead show evidence of relationships with Glanapteryginae (*sensu lato*).

In the process of comparisons, some other previously described species hitherto allocated in the genera *Ammoglanis* and *Stenolicmus* of Sarcoglanidinae, were found to be more closely related to the new taxa than to the type species of *Ammoglanis* and *Stenolicmus* or even to other Sarcoglanidinae. New generic allocations are proposed to attend to nomenclatural needs of the groups recognized. The aim of this paper is to report on the new taxa and to adjust the nomenclatural situation of the clades concerned so that the new forms can be meaningfully described. While it is not our purpose herein to resolve the broader ongoing phylogenetic conundrum, the taxa reported need to be made available, since they are certainly key elements in any upcoming efforts to tackle the situation with Glanapteryginae and Sarcoglanidinae. There is also a number of yet-unnamed species related to the new genera, and their taxonomic descriptions require a more coherent taxonomic framework. Thus, below we start with an essay on the new taxa, so that the new names can be used in the discussion that follows. Part of these findings have been anticipated in de Pinna (2016) and Reis (2023), with the latter explicitly proposing a monophyletic group composed of *Ammoglanis pulex* and *Stenolicmus ix* (herein placed in *Hyaloglanis* new genus and *Salpynx* new genus, respectively). We predict that the taxa established here will be important elements in resolving the complex taxonomic and phylogenetic situation in that region of the trichomycterid tree.

MATERIAL AND METHODS

Morphometric data were taken with digital calipers to the nearest 0.1 mm. Definition of measurements followed de Pinna & Dagosta (2022). Meristic data are expressed according to Bockmann & Sazima (2004), with fin-ray counts discriminating three types (unsegmented and unbranched represented by lower-case Roman numerals; segmented and unbranched by upper-case Roman numerals; and segmented and branched represented by Arabic numerals). The last posterior closely-set two rays in dorsal and anal fins were counted separately as branched rays (thus part of the Arabic numerals). Principal caudal-fin ray counts included all branched rays plus one unbranched ray in each lobe, counts given for each lobe (upper first) separated by a plus sign. Vertebrae numbers do not include those involved in the Weberian complex, and the compound caudal centrum was counted as one. Vertebral counts were taken from cleared and stained and radiographed material. Meristic and morphometric data were taken on the left side of specimens whenever possible.

Osteological data were obtained from specimens cleared and stained (CS) according to Taylor & van Dyke (1985), radiographs, and micro-tomography imaging. The latter was done with a Phoenix v|tome|x M – General Electric Company, using voxel size $X = 0.02370301$ microns, number of images 5000, voltage 60 Kv, and current 220 mA. Micro-tomographic images were processed using the software VG Studio Max, 2.2.3.69611 64 bit. Regular radiographs were taken with a Faxitron digital

x-ray system (https://volumegraphics.hexagon.com). Specimen dissection followed Weitzman (1974) with small changes to fit anatomical peculiarities of the Siluriformes. Osteological nomenclature followed de Pinna & Dagosta (2022). Glanapteryginae *sensu lato* (s.l.) refers to the traditional definition of the subfamily, *i.e.,* including *Listrura, Glanapteryx, Pygidianops,* and *Typhlobelus.* Glanapteryginae *sensu stricto* (s.s.) refers to the same assemblage exclusive of *Listrura* (which in this case is placed in Microcambevinae together with *Microcambeva*). Along the same lines, Sarcoglanidinae s.l. refers to the group composed of *Microcambeva, Malacoglanis, Sarcoglanis, Stauroglanis, Stenolicmus,* and *Ammoglanis* while Sarcoglanidinae s.s. is the same assemblage exclusive of *Microcambeva.*

Material examined

Comparative material used for this paper is listed below. Specimens at ZSM 25343 are inferred to be representatives of *Salpynx ix* or a close relative (see "Remarks" under description of genus *Salpynx* below). Generic reallocations proposed in this paper are adopted in the list below. Representatives examined of other Trichomycteridae and loricarioids are listed in de Pinna (1992).

Ammoglanis diaphanus, MZUSP 86249, 9 CS, 14.5-17.0 mm SL, Brazil, Mato Grosso, Cocalinho, rio Cristalino (rio Araguaia drainage). *Ammoglanis multidentatus,* UNT 10003, 7 (1 CS), 16.8-17.8 mm SL, Brazil, Bahia, Andaraí, rio Roncador. *Glanapteryx anguilla,* MZUSP 36530, 19 (2 CS), 33.7-63.2 mm SL, Brazil, Amazonas, Rio Negro, igarapé São João, near Tapurucuara, 00°24′S, 65°02′W. *Glanapteryx niobium,* INPA 12421, holotype, 55.3 mm SL, Brazil, Amazonas, Pico da Neblina National Park, Morro dos Seis Lagos, Lago Esperança, 00°17′N, 66°41′W. *Hyaloglanis pulex,* IAvH-P 15986, 38, 11.7-13.4 mm SL, Colombia, Vichada, Puerto Carreño, oxbow of caño Terecay, tributary of río Tomo (río Orinoco basin), 05°34′38.7″N, 68°29′39.8″W; IAvH-P 15987, 1, stream into to oxbow affluent to the internal lagoon of caño Terecay, tributary of río Tomo (río Orinoco basin), 05°34′37.5″N, 68°29′35.5″W; MZUSP 42471, paratypes, 21 (5 CS), 11.9-13.8 mm SL, Venezuela, Amazonas, Samariapo, río Paria Grande. *Listrura boticario,* MZUSP 128713, 4 (1 CS), 23.3-36.4 mm SL, Brazil, Paraná, Antonina, creek tributary to rio Copiava (rio Cachoeira drainage); MZUSP 69573, holotype, 1, 36.7 mm SL, Brazil, Paraná, pool adjacent to rio da Figueira (rio Guaraqueçaba drainage). *Listrura camposi,* MZUSP 95189, 17 (3 CS), 19.8-46.4 mm SL, Brazil, São Paulo, Pedro de Toledo, stream tributary to rio Itariri, rio Juquiá basin. *Listrura menezesi,* MZUSP 93882, 21 (2 CS), 12.3-32.6 mm SL, Brazil, Rio de Janeiro, Cachoeiras de Macacu, flooded area adjacent to rio das Panelas, rio São João basin, 22°35′19″S, 42°36′12″W. *Listrura nematopteryx,* MZUSP 36974, holotype, 26.9 mm SL, Brazil, Rio de Janeiro, Piabetá, marsh which joins Ribeirão Imbariê (tributary to rio Estrela); MZUSP 36975, paratypes, 12, 16.3-36.7 mm SL, collected with holotype; MZUSP 37138, 8 (CS), 14-28 mm SL, collected with holotype. *Listrura picinguabae,* MZUSP 106807, 6 (4 CS), 33.1-41.7 mm SL, Brazil, São Paulo, Ubatuba, coastal creek at Picinguaba. *Listrura tetraradiata,* MNRJ 19064, 10 (2 CS), 15.0-44.2 mm SL, Brazil, Rio de Janeiro, Saquarema, Palmital, Hotel Fazenda Barra da Castelhana. *Pygidianops amphioxus,* INPA 34661, holotype, 25.7 mm SL, Brazil, Amazonas, Manaus, Reserva Adolfo Ducke, igarapé do Acará, tributary to rio Tarumã, itself tributary to Rio Negro, 03°08′S, 60°02′W; MZUSP 87676, paratypes, 21 (2 CS), 23.3-30.4 mm SL, Brazil, Amazonas, rio Preto da Eva, igarapé Sucuriju, next to Bom Jesus farm, at km 13 of Ramal Francisca Mendes, 02°45′15.8″S, 59°37′29.6″W. *Pygidianops cuao,* MZUSP 81769 (ex-AMNH 232970), paratypes, 4 (1 CS), 13.4-19.0 mm SL, Venezuela, Amazonas, río Cuao at raudal Guacamaya, 8.1 miles upstream from raudal El Danto, 05°07.71′N, 67°31.53′W; MZUSP 82103, 5 (1 CS), paratypes, 13.4-19.0 mm SL, same data as MZUSP 81769; MZUSP 82104, paratypes, 3, 10.6-18.4 mm SL, Venezuela, Amazonas, río Cuao at isla de Cielo, 21.3 km upstream from raudal El Danto, 05°11.01′N, 67°31.11′W. *Pygidianops eigenmanni,* CAS 11121, paratypes, 2 (1 CS), 13.3-18.5 mm SL, Brazil, Amazonas, São Gabriel da Cachoeira, Rio Negro, rock pools below São Gabriel rapids. *Pygidianops magoi,* MZUSP 84303, paratypes, 2, 15.0-15.3 mm SL, Venezuela, Delta Amacuro, río Orinoco at Puerto Cabrian, 08°34′48″N, 62°15′54″W; MZUSP 84304, paratype, 1 CS, 11.4 mm SL, Venezuela, Bolívar, río Orinoco, 08°18.3′N, 62°56.1′W; MZUSP 84306, paratype, 1, 15.7 mm SL, Venezuela, Delta Amacuro, río Orinoco downstream from Puerto Cabrian, 08°34′N, 62°15′W. *Salpynx amapaensis,* ANSP 208058, 4, photos of live specimens and CT images of head, Brazil, Amapá, rio Mutura *ca.* 1 km upstream from confluence with Oyapock River, 02°35′14.5″N, 52°31′25.3″W; ANSP 209580, 1, photograph of live specimen, Brazil, Amapá, Igarapé Trilha 2, left bank tributary to rio Amapari, *ca.* 6.5 km north-northwest (upstream) from base camp, 01°14′20.2″N, 52°23′35.4″W. *Salpynx* cf. *ix,* ZSM 25343, 33 (4 CS), Brazil, Mission Tiryo, Serra Tumucumaque, rio Paru de Oeste; ZSM 28286, 4, Brazil, Pará, rio Trombetas basin, Igarapé Iveraca II, tributary of upper rio Paru de Oeste. *Stenolicmus sarmientoi* USNM 301664, paratype, 1 CS (disarticulated), 21.3 mm SL, Bolivia, Beni, Ballivia Province, río Matos (río Mamoré system). *Stenolicmus* sp. MZUSP 120578, 3, 15.7-27.6 mm SL, Brasil, Pará, Tailândia, rio Acará. *Typhlobelus guacamaya,* MZUSP 81770, paratypes, 3 (1 CS), 23.3-25.6 mm SL, Venezuela, Amazonas, río Cuao, at raudal Guacamaya, 13 km upstream from raudal El Danto, 05°07.71′N, 67°31.53′W. *Typhlobelus lundbergi,* MZUSP 84305, paratypes, 3 (1 CS), 20.8-22.0 mm SL, Venezuela, Bolívar, río Orinoco, 08°18′18″N, 62°56′06″W. *Typhlobelus macromycterus,* MNRJ 12129, holotype, 21.6 mm SL, Pará, rio Tocantins, near city of Tucuruí. *Typhlobelus* cf. *macromycterus,* MZUSP 106846, 5 (1 CS), 24.1-27.1 mm SL, Brazil, Pará, Belo Monte, paraná in rio Xingu, 03°06′06″S, 51°42′49″W. *Typhlobelus ternetzi,* CAS 11119, paratypes, 2 (1 CS, disarticulated), 22.3 mm SL, Brazil, Amazonas, São Gabriel da Cachoeira, Rio Negro, rock pools below São Gabriel rapids. *Typhlobelus* sp., INPA 36119, 2, 20.4-25.8 mm SL, Brazil, Pará, Senador José Porfírio, rio Xingu at Arroz Cru (*ca.* 03°33′S, 51°55′W).

RESULTS

Taxonomic accounts

Family Trichomycteridae
Salpynx, new genus
https://zoobank.org/FA7CDFB6-3305-4B5B-8C44-2B64032E5EC1

Type species: *Salpynx trombetensis,* new species.

Species included: *S. amapaensis* (Mattos, Costa & Gama, 2008), *Salpynx ephebus,* new species, *S. ix* (Wosiacki, Coutinho & de Assis Montag, 2011), and *S. trombetensis,* new species.

Diagnosis: Synapomorphically diagnosed by the posterior end of the barbular bone vertically expanded and bifurcated or bilobed and by the presence of a hypertrophied fenestra (here called a supratemporal fenestra) on the dorsal surface of the posterior part of the skull (framed by the pterotic and epioccipital anteromesially, the supracleithrum laterally and the margin of the Weberian capsule posteromesially), immediately anterior to the smaller orifice for the dorsal process of the cleithrum (Figs. 1-4). Further distinguished from putatively close relatives *Hyaloglanis* and *Potamoglanis* by the closed, entirely ossified skull roof (Figs. 1-3) (*vs.* skull roof open, occupied by one large fontanel, Fig. 5). Further distinguished from most species of *Hyaloglanis* by the presence of a well-developed barbular bone (Figs. 1-4) (*vs.* absent or vestigial, except in *H. nheengatu*); by the body opaque and with heavy integumentary dark pigmentation (Fig. 6) (*vs.* body translucent and with reduced integumentary dark pigmentation, combined with internal pigmentation in the sagittal plane of body visible by transparency in the live fish; Fig. 7); by the cephalic latero-sensory canal entering sphenotic (*vs.* restricted to pterotic). *Salpynx* differs further from *Potamoglanis* by the cephalic latero-sensory canal system not extending anteriorly beyond sphenotic (*vs.* extending to frontal and nasal). *Salpynx* shares exclusively with *Hyaloglanis* and *Potamoglanis:* lateral ethmoids narrow and curved towards midline anteriorly, forming arc separated by wide space, contacting each other only anteriorly and bracing posterior portion of ethmoid cartilage at that portion only (Figs. 3, 5); and parasphenoid anteriorly expanded as a wide lamina to fill space of braincase floor between receded portion of lateral ethmoids (Figs. 3, 5). Other characters useful for identification include a reduced posterolateral process of the palatine oriented at right angle laterally to main axis (longitudinal) of bone, and the lack of latero-sensory canals in the frontals and further anteriorly (Figs. 1-5, 8).

Etymology: From the Greek salpinx, meaning a type of horn or trumpet, in allusion to the rio Trombetas (locality of the type species of the genus), which has the same meaning in Portuguese. The use of "y" is intended to avoid allusion to a similar medical-anatomical term. Gender feminine.

Remarks: The original description of *Salpynx ix* was based on the then unique holotype. As a consequence, its inclusion in *Stenolicmus* and in Sarcoglanidinae was based exclusively on externally-observable characteristics. Indeed, *S. ix* (Fig. 9) shares some general body shape and meristic similarities with the type species of *Stenolicmus, S. sarmientoi*. It also has a totally closed skull roof (*i.e.,* no cranial fontanels) and comparatively heavy integumentary dark pigmentation. Specimens ZSM 25343 and 28286 examined here (Fig. 9) are inferred to be representatives of *Salpynx ix* or a close relative. Although additional data on the species is needed for a definitive identification, the specimens match the holotype in nearly all characteristics which are available in the original description (Wosiacki *et al.,* 2011). In particular, ZSM specimens display a hypertrophied maxillary-barbel base (Fig. 9), a trait which matches that of the holotype (cf. Wosiacki *et al.,* 2011, fig. 3) but which contrasts with the less pronounced situation seen in other species of *Salpynx*. One of the few discrepancies is that only postotic sensory pores 1 to 2 are present in the skull according to Wosiacki *et al.* (2011). The ZSM specimens have an additional small otic pore anteriorly to postotic 1 (exiting from the middle of the sphenotic). That pore is minute and we find it plausible that it was not visible in the unique type of the species at the time of description. We thus conclude that specimens in ZSM 25343 and 28286 are either *S. ix* or a closely related form. Geographically, the ZSM specimens come from the rio Paru de Oeste, a basin adjacent to the rio Curuá, type locality of *S. ix*. Internal anatomical data on those specimens leave no doubt that they are representatives of *Salpynx* as defined here, and not of *Stenolicmus*. They lack all synapomorphies so far proposed for the subfamily and which are well documented in the type species of *Stenolicmus, S. sarmientoi* (de Pinna & Starnes, 1990). Also, characters included in the phylogenetic scheme advanced here support that it belongs in a monophyletic group together with other species of *Salpynx*. Specimens USNM 409756 (from Surinam, upper Paloemeu river, near the border of Brazil) are identified as *Stenolicmus ix* in Ferrer (2016). As in the previous case, they are definitely members of *Salpynx* as per illustrations of their internal anatomy in Ferrer (2016, figs. 13, 19A, 27, 34 to 40). While their premaxillary dentition visible in illustrations leaves no doubt that they are neither *S. trombetensis* nor *S. ephebus,* the presence of an ossification on the anterior palatine cartilage (Ferrer, 2016, fig. 13) fits the condition reported for *S. amapaensis* and not that of presumed *S. ix* ZSM specimens reported above, which lack such ossification. Resolution of the specific identity of USNM 409756 material will require data on the internal anatomy of the holotype of *S. ix*.

Salpynx trombetensis, new species
(Fig. 10)
https://zoobank.org/C82EBA9A-65C0-498D-83B0-EE738699ED2F

Trichomycterus sp. 2; Ferreira, 1993: 54 [list; geographical provenance; description of general area].

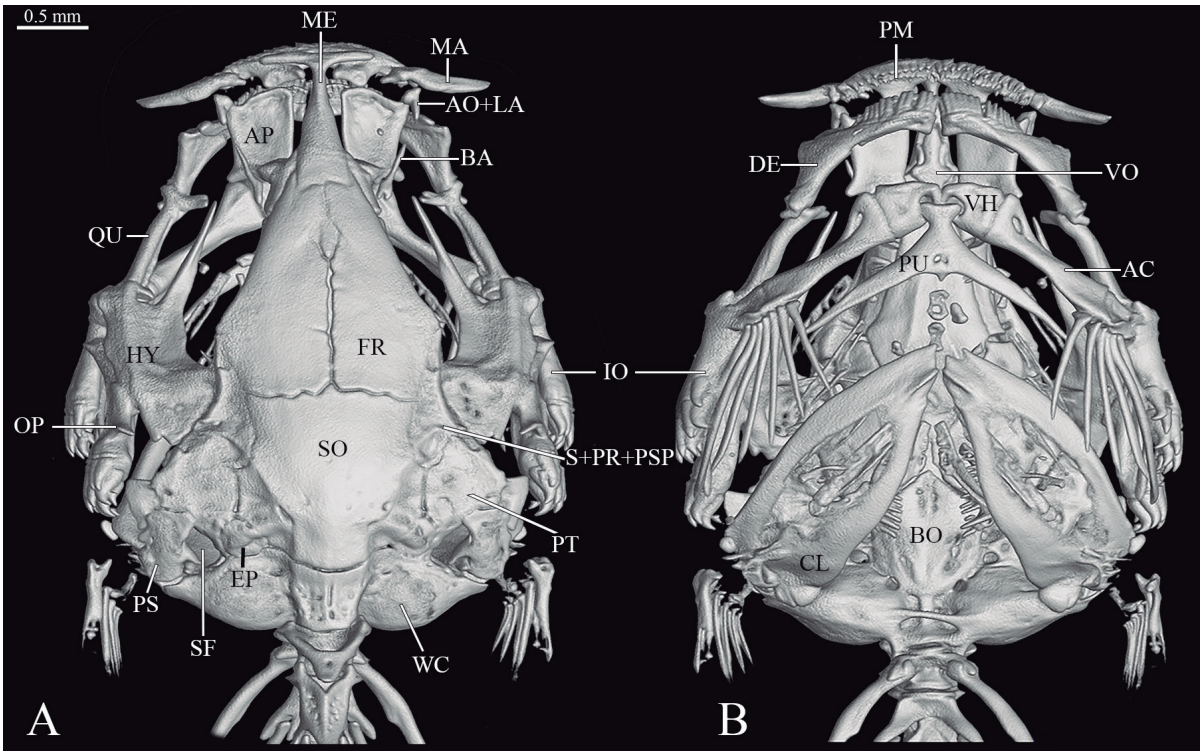

Figure 1. *Salpynx trombetensis,* holotype INPA 13021, CT-scan images of head, (A) dorsal view, (B) ventral view. Scale bar = 0.5 mm. Abbreviations: AC, anterior ceratohyal; AP, palatine; AO+LA, lacrimal-antorbital; BA, barbular; BO, basioccipital; CL, cleithrum; DE, dentary; FR, frontal; HY, hyomandibula; IO, interopercle; MA, maxilla; ME, mesethmoid; OP, opercle; PM, premaxilla; PS, supracleithrum; PT, pterotic; PU Parurohyal; SF, supratemporal fenestra; S+PR+PSP, sphenotic-prootic-pterosphenoid; QU, quadrate; SO, supraoccipital; VH, ventral hipohyal; VO, vomer; WC, Weberian capsule.

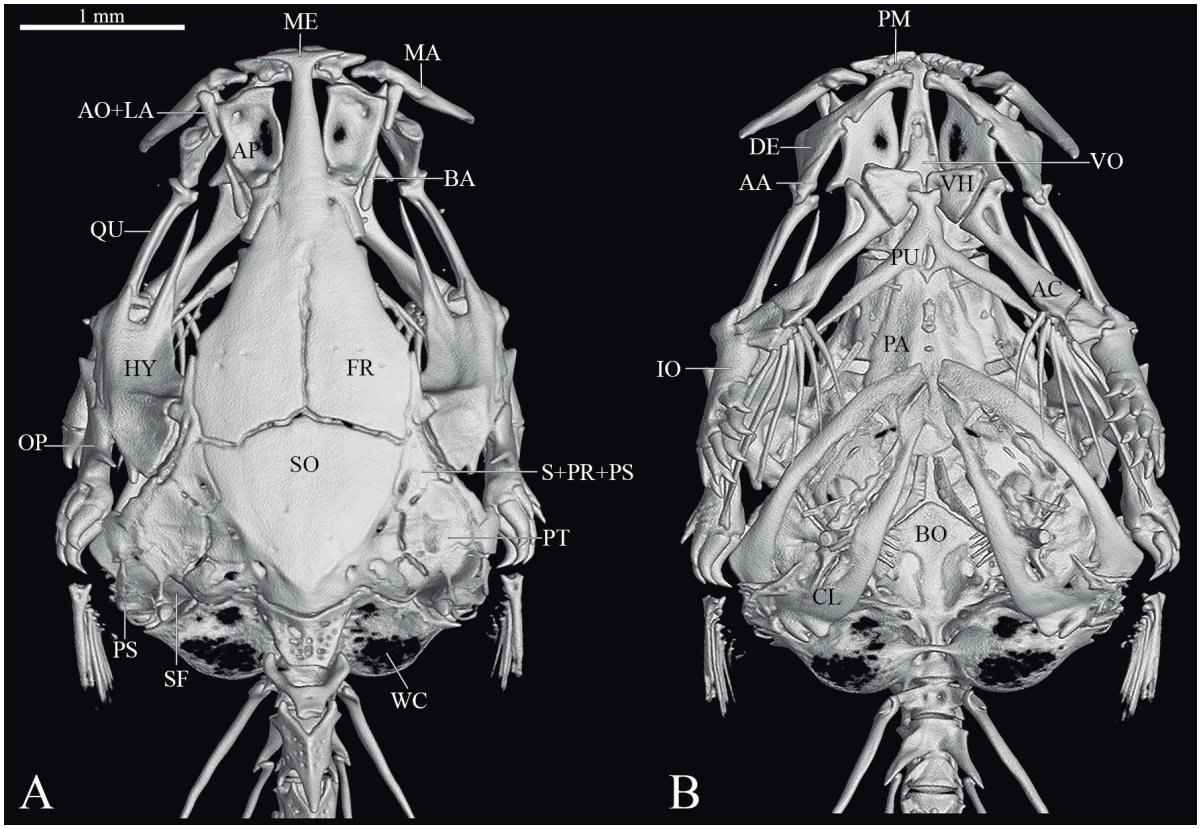

Figure 2. *Salpynx ix,* ZSM 28286, CT-scan images of head, (A) dorsal view, (B) ventral view. Scale bar = 1 mm. Abbreviations: AA, anguloarticular; AC, anterior ceratohyal; AP, palatine; AO+LA, lacrimal-antorbital; BA, barbular; BO, basioccipital; CL, cleithrum; DE, dentary; EP, epioccipital; FR, frontal; HY, hyomandibula; IO, interopercle; LE, lateral ethmoid; MA, maxilla; ME, mesethmoid; OP, opercle; OS, orbitosphenoid; PA, parasphenoid; PM, premaxilla; PT, pterotic; PS, supracleithrum; SO, supraoccipital; SF, supratemporal fenestra; S+PR+PS, sphenotic-prootic-pterosphenoid; VH, ventral hypohyal; VO, vomer; WC, Weberian capsule.

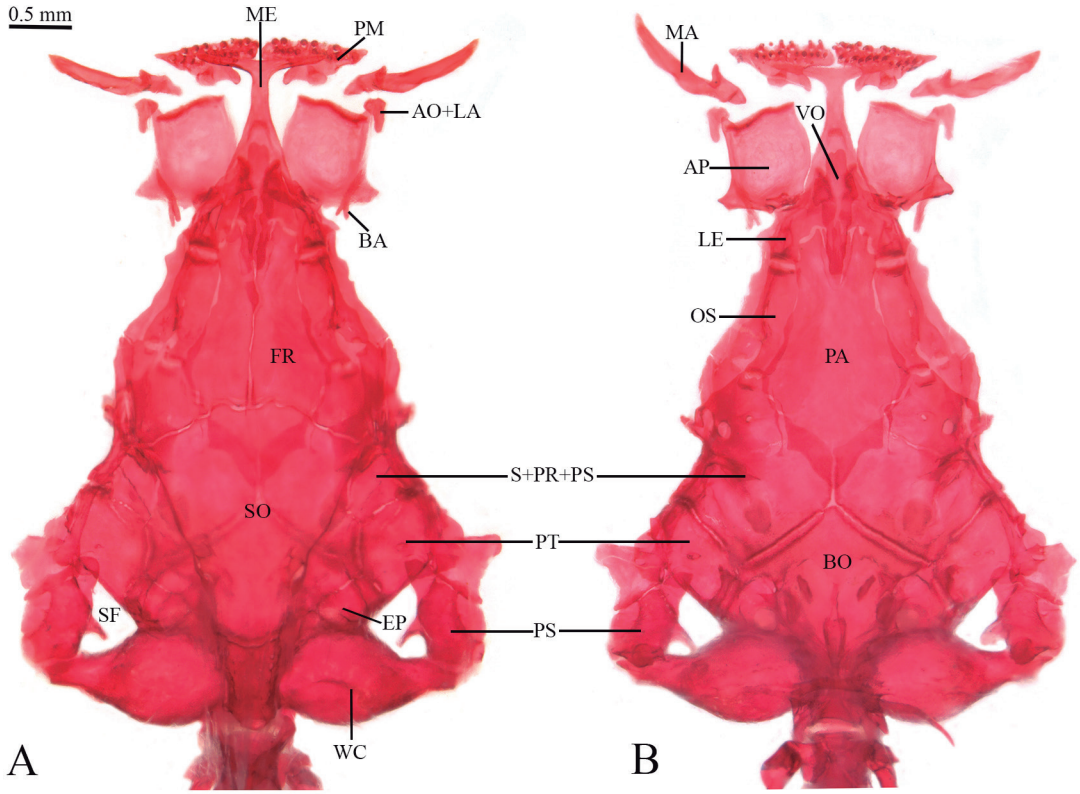

Figure 3. *Salpynx ephebus,* paratype INPA 52374, CS specimen, head, (A) dorsal view, (B) ventral view. Scale bar = 0.5 mm. Abbreviations: AP, palatine; AO+LA, lacrimal-antorbital; BA, barbular; BO, basioccipital; EP, epioccipital; LE, lateral ethmoid; FR, frontal; MA, maxilla; ME, mesethmoid; OS, orbitosphenoid; PA, parasphenoid; PM, premaxilla; PT, pterotic; PS, supracleithrum; SO, supraoccipital; SF, supratemporal fenestra; S+PR+PS, sphenotic-prootic-pterosphenoid; VO, vomer; WC, Weberian capsule.

Holotype: INPA 61216, 21.8 mm SL, Brazil, Pará, Município de Oriximiná, unnamed igarapé at km 14 of road BR-163 (from Cachoeira Porteira to road BR-210 or Perimetral Norte) (00°58′47″S, 56°59′25″S), *ca.* 68 masl., rio Trombetas drainage, E. Ferreira and J. Zuanon, 06 Dec 1988.

Paratypes (all collected with holotype): INPA 13021, 27, 18.9-24.6 mm SL; MZUSP 130909, 10 (4 CS), 19.6-22.5 mm SL.

Diagnosis: Distinguished from all congeners by having 32-37 premaxillary teeth (*vs.* 17-21 in *S. ephebus,* 10-12 in *S. ix;* 8-11 in *S. amapaensis*); by the premaxillary teeth arranged in two rigidly regular rows forming arc across two premaxillae (Fig. 11A; *vs.* two irregular rows or single row in straight formation or irregular line, Fig. 11B, C); by having 33-34 dentary teeth (*vs.* 20-22 in *S. ephebus,* 12-15 in *S. ix;* 7-8 in *S. amapaensis*); by having dentary teeth disposed in three regular wavy rows (with anterior row short, near symphysis only) and teeth gradually larger towards symphysis in each row (*vs.* two rows, with teeth similar-sized along each row); and by the sphenotic branch of the latero sensory canal running through nearly entire length of bone. Further distinguished from *S. ix* and *S. amapaensis* by having three ribs (*vs.* two); and by the maxilla strongly deflected anteriorly and approximately as long as the anterior margin of the premaxilla (*vs.* maxilla mostly straight and at least twice as long as the anterior margin of the premaxilla). Further distinguished from *S. ix* by the posterior naris located much closer to eye than to anterior naris (distance between posterior and anterior nares 1.5-2.0 times that between posterior naris and eye, Fig. 10; *vs.* posterior naris equidistant between eye and anterior naris or closer to anterior naris than to eye).

Description: Morphometric data are provided in Table 1. Overall body shape shown in Fig. 10. Body short,

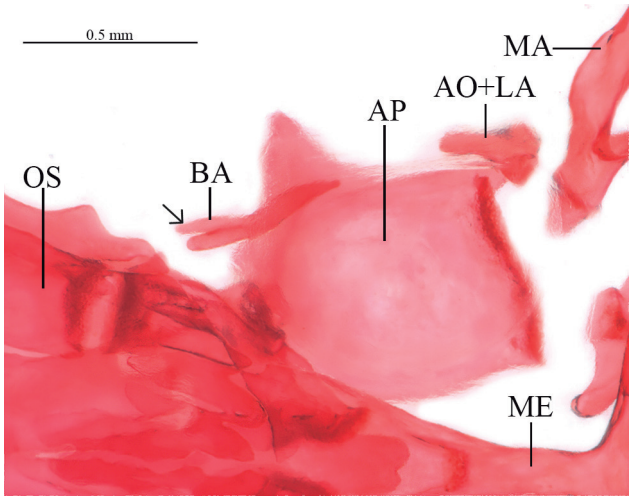

Figure 4. *Salpynx ephebus,* INPA 52374, CS specimen, partial view of anterior portion of skull and associated structures, dorsal view, left side, anterior to right. Scale bar = 0.5 mm. Abbreviations: AO+LA, lacrimal-antorbital; BA, barbular; AP, palatine; MA, maxilla; ME, mesethmoid; OS, orbitosphenoid. Arrow: bifurcated barbular.

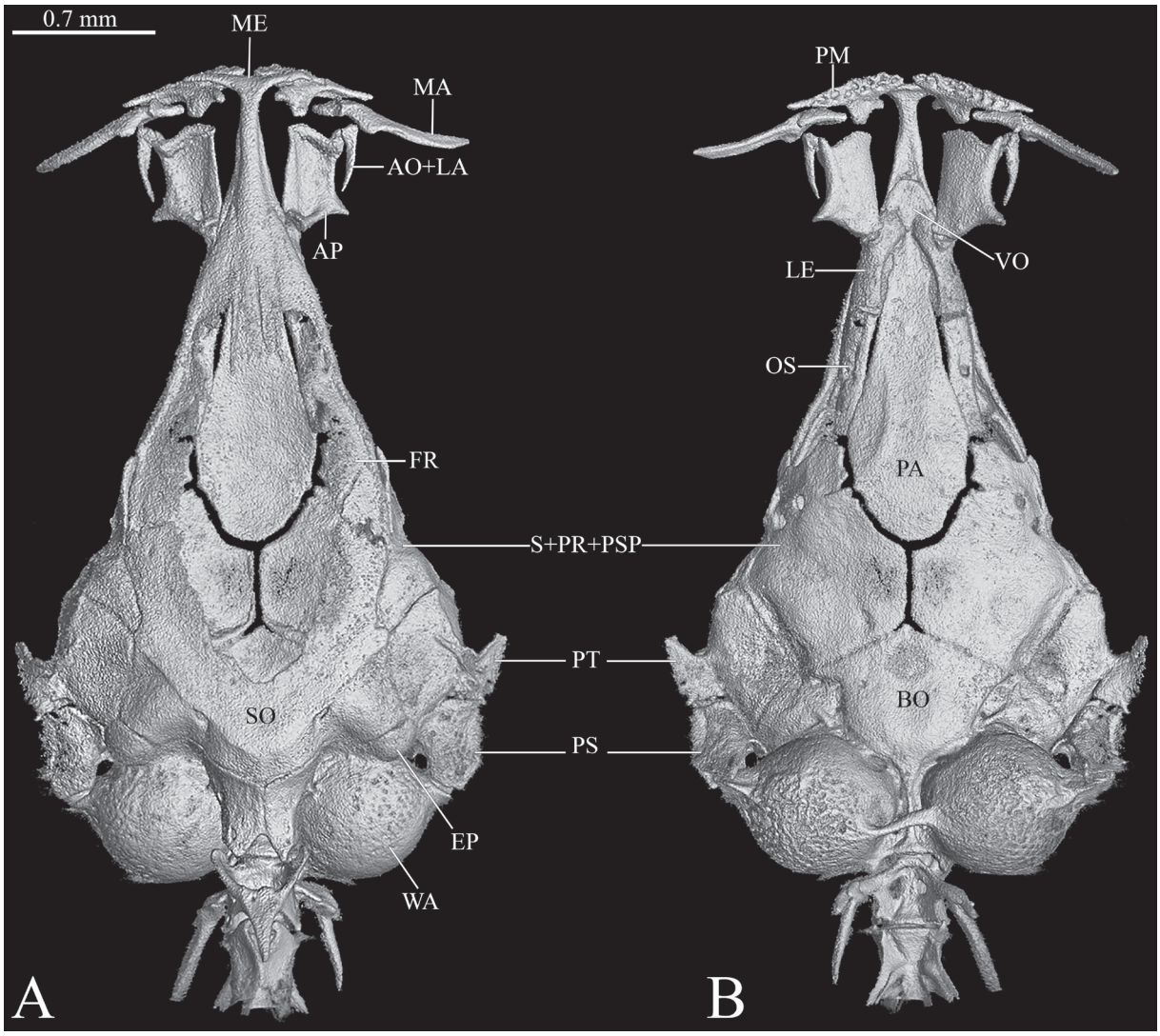

Figure 5. *Hyaloglanis pulex,* MZUSP 42471, CT-scan images of head, (A) dorsal view, (B) ventral view. Scale bar = 0.7 mm. Abbreviations: AO+LA, lacrimal-antorbital; AP, palatine; BO, basioccipital; EP, epioccipital; FR, frontal; LE, lateral ethmoid; MA, maxilla; ME, mesethmoid; OS, orbitosphenoid; PA, parasphenoid; PM, premaxilla; PT, pterotic; PS, supracleithrum; S+PR+PSP, sphenotic-prootic-pterosphenoid; SO, supraoccipital; VO, vomer; WA, Weberian capsule.

Figure 6. Color variation in live specimens (A and B) of *Salpynx amapaensis,* ANSP 208058, in lateral view. Photographs by Mark Sabaj.

Figure 7. Live specimens of *Hyaloglanis pulex,* IAvH-P 15986. Photograph by Felipe Villegas.

head wider than trunk in dorsal view. Body slightly depressed at pectoral-fin insertion, then deeper than wide immediately posterior and gradually more compressed posteriorly, tapering to caudal fin. Dorsal profile of head straight or gently convex, continuous with body or separated from it by slight lump. Dorsal profile of trunk forming straight or broadly convex arc from occiput to dorsal-fin origin. Base of dorsal fin straight, declining to caudal peduncle. Dorsal and ventral margins of caudal peduncle straight and parallel, continuous with caudal fin, in some specimens slightly expanded on posterior half. Most of dorsal and ventral margins of caudal peduncle formed by low cutaneous fold, supported by procurrent ray series. Ventral profile of head straight or gently convex. Ventral profile of body straight (ventrally flattened) immediately posterior to head, then slightly convex (in specimens with distended abdomen) to anal fin. Base of anal fin straight, ascending to caudal peduncle.

Table 1. Morphometric data of *Salpynx trombetensis* **sp. nov.** (n = 6)

	Holotype	Range	Mean	SD
Standard length (mm)	22	21.7-23.5	22.3	0.8
% of standard length				
Anal-fin base	6.4	5.5-9.9	7.1	1.8
Body depth	17.3	13.8-18.5	17.0	1.7
Caudal peduncle depth	11.8	11.5-12.9	12.0	0.6
Dorsal-fin base	6.8	5.2-8.1	6.8	1.2
First pectoral-fin ray length	18.6	18.6-23.8	21.6	2.0
Head length	17.7	17.7-19.4	18.5	0.6
Preanal length	67.3	67.3-77.9	73.9	3.7
Predorsal length	64.7	64.7-73.6	70.7	3.7
Prepelvic length	60.8	60.8-65.6	62.9	2.0
% of head length				
Eye diameter	8.2	8.1-10	9.1	0.7
Interorbital width	28.2	21.4-28.2	25.4	2.5
Snout length	46.2	37.2-46.2	40.9	3.3
Mouth width	46.2	42.9-46.5	44.7	1.4

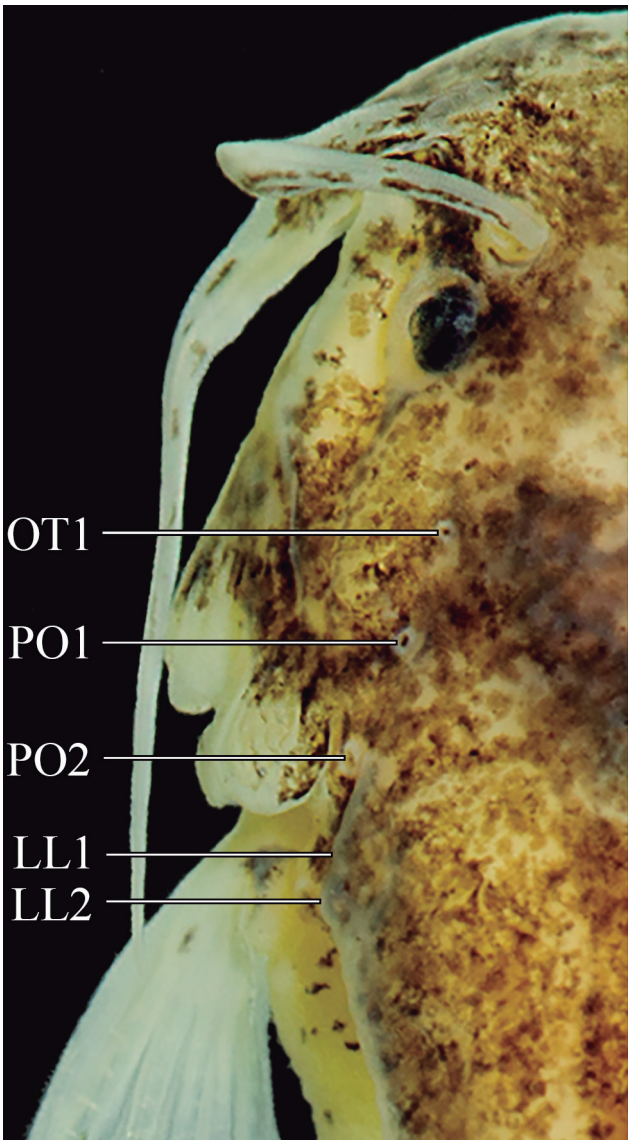

Figure 8. Close-up view of head left side of *Salpynx ephebus* showing sensory pores. Abbreviations: OT1, otic pore 1; PO 1-2, postotic pore 1 to 2; LL 1-2, lateral line pores 1-2.

Figure 9. *Salpynx ix,* ZSM 28286, 20.2 mm SL. (A) lateral view; (B) dorsal view of head and anterior trunk; (C) ventral view of head and anterior trunk.

Figure 10. *Salpynx trombetensis,* new species, holotype INPA 61216, 21.8 mm SL, (A) lateral view; (B) dorsal view of head and anterior trunk; (C) ventral view of head and anterior trunk.

Head depressed, less deep than any part of body (Fig. 10). Branchial membranes narrowly united to anterior part of isthmus, gill openings wide, unconstricted. Eye small but well formed, with distinct lens and covered by thin transparent integument, located dorsally on head, with small lateral component, anterior to middle of HL. Anterior naris round, positioned closer to anterior margin of snout than to anterior margin of eye, surrounded by tube of integument continuous posterolaterally with nasal barbel. Anterior internarial distance variable, ranging from slightly less to slightly more than interorbital. Posterior naris round, smaller than eye, located much closer to eye than to anterior naris, posterolaterally separated from eye by narrow area of soft tissue equivalent half orbital diameter or slightly less. Short semilunar flap of integument along anterior margin of posterior naris. Posterior internarial distance shorter than anterior internarial distance, slightly larger than 50% of interorbital. Mouth subterminal, wide, upper jaw slightly longer than lower, margin of lower jaw straight or gently convex. Upper lip continuous with remainder of dorsal surface of head and base of maxillary barbel. Lower lip narrow, forming peculiar laterally long narrow lobes well differentiated from remainder of ventral surface of head, nearly meeting at midline. Lobes separated from base of rictal barbel on each side by abrupt soft tissue bend. Integument of both lips smooth under superficial examination, papillae not visible probably due to long preservation history. Premaxillary teeth 32-37, conical, arranged in two rigidly regular rows in gentle arc across both premaxillae (Fig. 11A; 14-17 on anterior row and 17-20 on posterior one), with those on posterior row more closely-set than on anterior one. Both rows distributed along entire anterior margin of bone. Dentary teeth 33-34, conical, in three regular wavy rows (5-7 on short anterior row near symphysis, 13-14 on second, 14-15 on third), with individual teeth increasing in size towards symphysis. Three pairs of barbels well devel-

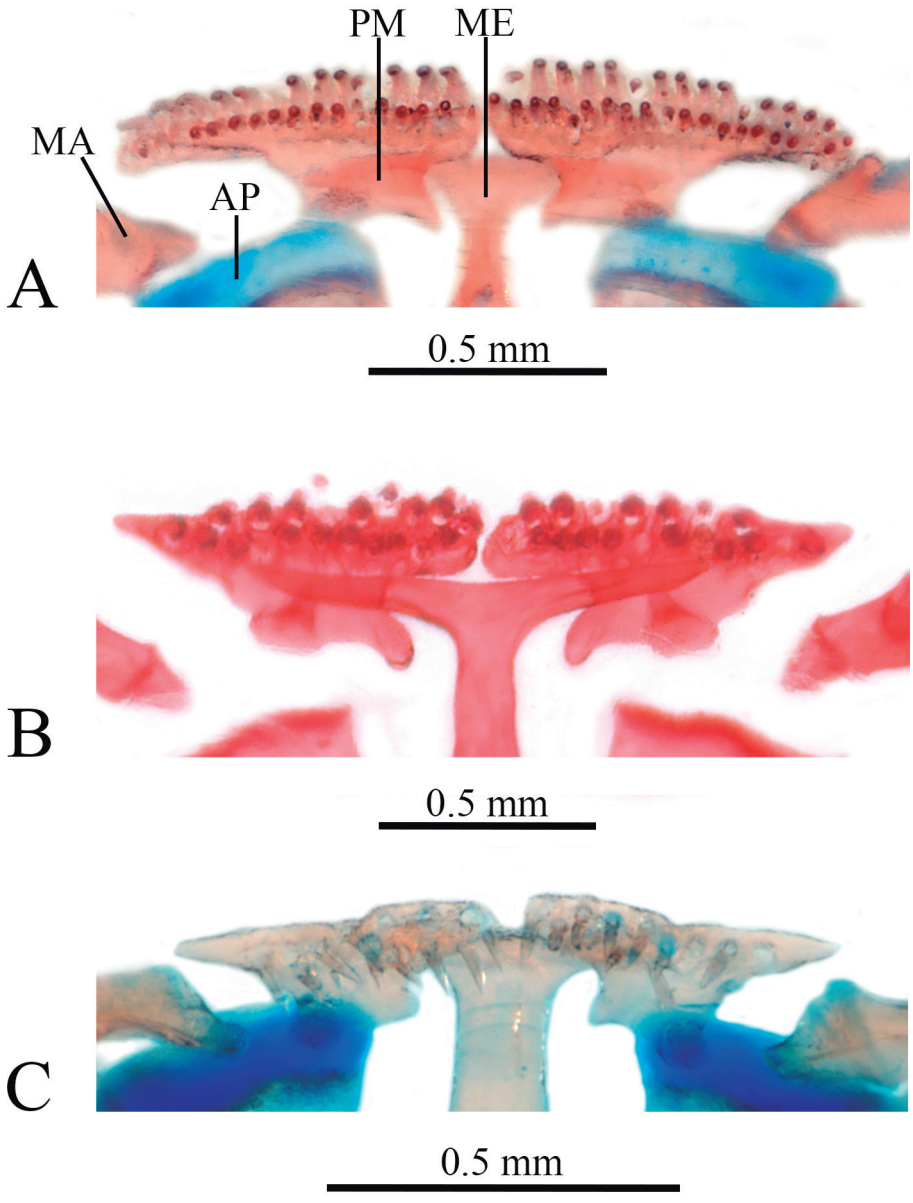

Figure 11. Ventral view of premaxillae and associated structures of *Salpynx.* (A) *Salpynx trombetensis* paratype, MZUSP 130909; (B) *S. ephebus,* paratype, INPA 52374; (C) *S. ix,* ZSM 25343. Abbreviations: AP, palatine; MA, maxila; ME, mesethmoid; PM, premaxilla.

oped, with visible internal cores, particularly on maxillary barbel. Base of maxillary barbel broad but continuous with soft portion of barbel, its maximum width less than distance of its posterior margin to eye, distal portion of maxilla entering only basal portion of barbel base. Distance between abducted fleshy maxillary barbel bases less broad than head width (Fig. 10). Extended maxillary barbel variably reaching to posterior margin of opercular odontodophore or to slightly beyond end of pectoral-fin base. Rictal barbel shorter than maxillary barbel, attached to corner of mouth, its base covered dorsally by maxillary barbel base, variably reaching to middle of interopercular odontodophore to margin of branchiostegal membrane when extended. Nasal barbel approximately as long as other barbels, reaching to transverse line through end of opercular odontodophore or slightly beyond. Opercular odontodophore small, round, located immediately anterior to pectoral-fin origin in dorsal projection, surrounded by narrow periodontodal fold (Fig. 10). Nine or ten opercular odontodes (anterior one or two small) clustered in roundish arrangement. Interopercular odontodophore oblong, varying in size from slightly larger than opercular odontodophore to twice its total area, ventrolateral on head, surrounded by uniformly narrow periodontodal fold. Twelve to fourteen interopercular odontodes disposed in two irregular rows.

Lateral line reduced to tiny canal dorsal to pectoral-fin base split in two equaly short branches each opening as terminal pore. Single short and poorly ossified canal bone on dorsal branch. Sensory canal running anteriorly through supracleithrum, pterotic and most of sphenotic. Three cephalic latero-sensory pores, one near anterior terminus of sphenotic, another at junction sphenotic-pterotic and one at junction pterotic-supracleithrum. Anterior pore (representing anterior terminus of latero-sensory system) posterior to eye and distant from latter by one-and-a-half eye diameter or slightly more. Frontals lacking sensory canal. Nasal branch of latero-sensory system (and bone) absent.

Pectoral fin long, narrow, originating immediately posterior to posterior margin of branchial membrane, slightly anterior to vertical through posterior margin of opercular odontodophore (Fig. 10). Pectoral-fin rays I+4, with last ray always branched. Branched rays splitting once. First pectoral-fin ray (unbranched), markedly longer and thicker than other rays, prolonged as a long filament extending beyond rest of fin by 50-100%. Other rays progressively shorter and thinner, all protruding slightly beyond fin membrane. Pelvic fin small, elongate, its origin posterior to middle of SL, well anterior to vertical through origin of dorsal fin; its posterior end entirely covering anal and urogenital openings, reaching or nearly reaching fleshy origin of anal fin, but not base of first anal-fin ray. Pelvic-fin rays I+3*, I+2+I or I+3+I, all segmented, first and second branched rays longest. Pelvic splint present, extending for approximately basal one-fifth of first segmented ray. Bases of pelvic fins separated by narrow space. Dorsal fin oblong, with round distal margin, its origin on posterior half of SL, anterior to vertical through anal-fin origin and slightly anterior to vertical through end of pelvic fin. Dorsal-fin rays i+II+5 (7), i+II+4+I (7*), i+III+3+I (1), i+III+4 (1), first and second branched rays longest, branched rays splitting once. Anal-fin oblong, similar in shape and size to dorsal fin, its origin at or slightly posterior to end of pelvic fin, posterior to vertical though middle of dorsal-fin base. Anal-fin rays i+II+4 (10*), i+II+3+I (4), II+4 (1), second branched ray longest, branched rays splitting once. Caudal fin slightly longer than deep, slightly deeper than caudal peduncle when expanded. Caudal-fin margin damaged in all available specimens, apparently gently convex, nearly truncate with round corners. Caudal-fin rays 5+6 (2), 6+5 (1), 6+6 (12*), all principal rays with similar lengths except slightly shorter upper-most and lower-most ones, branched rays splitting once. Procurrent caudal-fin rays nine or ten dorsally and eight or nine ventrally, extending for posterior third or slightly more of caudal peduncle length and merging gradually into principal caudal rays.

Axillary gland small, visible as tumescent area posterodorsal to base of pectoral fin, with small translucent core immediately posterior to pectoral-fin base in some specimens. Gland pore small, located anteriorly on gland, axillar in position relative to pectoral fin base, posteroventral to far more visible sensory pore exiting from supracleithrum. Gland pore collapsed as slit in most specimens, filled to surface with coagulated mucus.

Vertebrae 32 or 33. First dorsal-fin pterygiophore posterior to neural spine of vertebra 16 or 77. First anal-fin pterygiophore aligned with hemal spine of vertebra 17 or 88. Ribs three. Branchiostegal rays six. Seven dorsal- and six anal-fin pterygiophores. Cranial fontanels absent.

Pigmentation in alcohol (Fig. 10): Specimens in advanced stage of fading, but with following features still visible. Dorsum and flanks with large irregular, mostly roundish, dark spots, arranged in poorly defined longitudinal bilateral rows, one along dorsal margin of body and another along midlateral line. Spots interspersed with, and partly overlain by, irregularly-distributed individual chromatophores. Caudal peduncle with same covering as rest of body, with vague outlining of posterior myotomes on posterior region of caudal peduncle. Dorsal surface of head with spots similar yet smaller than those on dorsum, combining with underlying brain pigment on posterior part of braincase. Dark chromatophores concentrated along margins of braincase, region between eyes and nares and lateral to latter. Small area ventrolateral to eyes lacking dark chromatophores. Dark concentrations on cheeks and dorsal margin of opercular odontodophore. Ventral portion of head mostly white, with faint dark clouds over base of interopercular odontodophore. Dorsal surface of pectoral-fin base with concentration of dark chromatophores, sometimes forming dark irregular spot. Base of dorsal fin with dark concentration, extending sparsely onto basal part of fin web of former. Pelvic fin hyaline. Base of caudal fin with vertical dark arc crossing principal and accessory rays immediately posterior to their bases, along posterior limit of hypural plate, darkest at hypural diastema. Remainder of caudal fin white or with sparse dark markings.

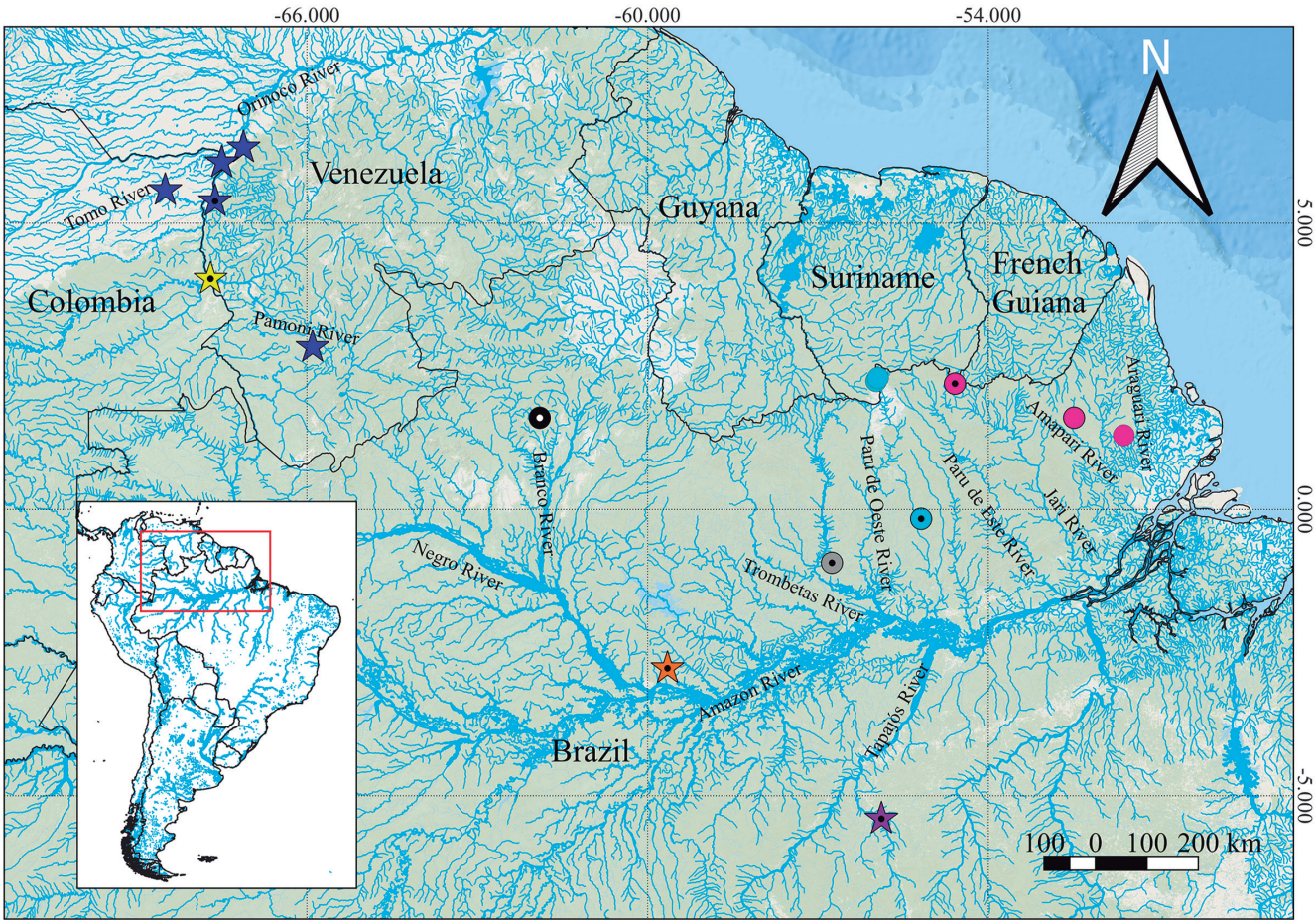

Figure 12. Geographical distribution of *Salpynx* and *Hyaloglanis* species. Star means *Hyaloglanis;* circle means *Salpynx;* dotted symbols mean holotypes. Colors: yellow = *H. natgeorum;* purple = *H. nheengatu;* orange = *H. obliquus;* dark blue = *H. pulex;* light blue = *S. ix;* grey = *S. trombetensis;* black = *S. ephebus;* pink = *S. amapaensis.*

Geographical distribution (Fig. 12): *Salpynx trombetensis* is known exclusively from an unnamed lowland Terra Firme igarapé flowing directly into the left margin of the lower Rio Trombetas at an altitude of 68 masl. The locality is in the Brazilian State of Pará, Municipality of Oriximiná.

Ecological notes: According to E. Ferreira (*pers. comm.*), *Salpynx trombetensis* was collected in a small *terra firme* stream (5-6 m wide), with clear water, moderate current, sandy substrate with interspersed rocks and low vegetation along margins. The part of the stream close to the road was somewhat impacted due to construction work, but entered pristine forest a few meters in either direction. The specific microhabitat is unknown since collection was done with rotenone. *Salpynx trombetensis* occurs in low-altitude range (*ca.* 70 masl) but in terra firme terrain, above the first waterfall of the rio Trombetas. Other species collected at the same place and event were Loricariidae: *Lasiancistrus* sp., *Paralithoxus stocki, Rineloricaria* gr. *formosa;* Heptapteridae: *Rhamdia* sp.; Erythrinidae: *Hoplias aimara, Hoplias* sp.; Lebiasinidae: *Pyrrhulina laeta;* Acestrorhamphidae: *Astyanax clavitaeniatus, Jupiaba acanthogaster, Moenkhausia surinamensis, Poptella brevispina;* Iguanodectidae: *Bryconops affinis;* Cichlidae: *Aequidens tubicen;* Rivulidae: *Rivulus* sp. The general area and collection project during which *S. trombetensis* was found is described in Ferreira (1993), where the species is listed as *Trichomycterus* sp. 2.

Etymology: Trombetensis is an allusion to the major basin where the species is found, the rio Trombetas. The sufix -ensis is a 3rd-declension adjective, invariant for all genders.

Salpynx ephebus, new species
(Fig. 13)
https://zoobank.org/22AAAAE2-30DE-4DF3-9F3C-56B13B786FDE

Holotype: INPA 61217, 30.5 mm SL, Brazil, Roraima, Caracaraí, Serra da Mocidade, unnamed igarapé into rio Pacu (rio Branco drainage), *ca.* 1,000 m along eastern trail, 01°36′0.99″N, 61°54′00.16″W, 638 masl, D.A. Bastos, G.G. Barros and P.M. Ito, 17 Jan 2016.

Paratypes (all collected with holotype): INPA 52374, 20, 15.0-30.2 mm SL; INPA 52374, 2 CS, 17.3-29.4 mm SL; MZUSP 130910, 7, 17.6-29.8 mm SL.

Diagnosis: Distinguished from all congeners by having 17-21 premaxillary teeth (*vs.* 32-37 in *S. trombetensis,* 10-12 in *S. ix;* 8-11 in *S. amapaensis*); by having 20-22 dentary teeth (*vs.* 33-34 in *S. trombetensis,* 12-15 in *S. ix;*

7-8 in *S. amapaensis*), and by having premaxillary teeth arranged in two irregular rows (*vs.* single row in *S. ix* and *S. amapaensis* and three rows in *S. trombetensis*). Further distinguished from *S. ix* and *S. amapaensis* by having three ribs (*vs.* two); and by the maxilla strongly deflected anteriorly and approximately as long as the anterior margin of the premaxilla (*vs.* maxilla mostly straight and at least twice as long as the anterior margin of the premaxilla). Further distinguished from *S. trombetensis* by the premaxillary teeth arranged in irregular rows (*vs.* rows rigidly regular forming arc) and by the sphenotic branch of the latero sensory canal running through posterior part of bone only (*vs.* running through entire length of bone). Further distinguished from *S. ix* by the posterior naris located much closer to eye than to anterior naris (distance between posterior and anterior nares 1.5-2.5 times that between posterior naris and eye; *vs.* posterior naris equidistant between eye and anterior naris or closer to anterior naris than to eye).

Table 2. Morphometric data of *Salpynx ephebus* **sp. nov.** (n = 12)

	Holotype	Range (12)	Mean	SD
Standard length (mm)	30.9	21.9-30.9	25.2	3.2
% of standard length				
Head length	16.5	16.5-19.6	18.3	0.8
Dorsal-fin base	7.3	7.3-10.2	9.5	0.8
Anal-fin base	8.4	7.1-10	9.0	0.8
Body depth	13.0	13-16.9	14.7	1.1
Caudal peduncle depth	10.8	10.8-13.2	12.1	0.6
First pectoral-fin ray length	18.0	16.9-26.9	21.4	2.9
Preanal length	67.8	66.2-73.8	69.9	2.2
Predorsal length	66.0	63.1-73.5	67.6	2.8
Prepelvic length	56.0	56-62.4	59.7	1.7
% of head length				
Eye diameter	11.6	10.5-12.5	11.6	0.6
Interorbital width	33.3	28.9-37.5	32.7	2.3
Snout length	38.2	29-41	35.5	3.2
Mouth width	47.1	40.9-50	44.8	3.0

Description: Morphometric data provided in Table 2. Overall body shape shown in Fig. 13. Body short, head wider than trunk in dorsal view. Body slightly depressed at pectoral-fin insertion, then deeper than wide immediately posterior and gradually more compressed posteriorly, tapering to caudal fin. Dorsal profile of head straight or gently convex, generally continuous with body. Dorsal profile of trunk sometimes separated from that of head by slight lump, then straight or broadly convex arc from occipital to dorsal-fin origin. Base of dorsal fin straight, declining to caudal peduncle. Dorsal and ventral margins of caudal peduncle straight and parallel, continuous with caudal fin, in few specimens slightly converging or diverging near caudal fin. Most of dorsal and ventral margins of caudal peduncle formed by low cutaneous fold, supported by procurrent ray series. Ventral profile

Figure 13. *Salpynx ephebus,* new species, holotype INPA 61217, 30.5 mm SL, (A) lateral view; (B) dorsal view of head and anterior trunk; (C) ventral view of head and anterior trunk.

of head straight or gently convex. Ventral profile of body straight (flattened) immediately posterior to head, then straight or slightly convex (in specimens with distended abdomen) to anal fin. Base of anal fin straight, ascending to caudal peduncle.

Head depressed, less deep than any part of body. Branchial membranes narrowly united to anterior part of isthmus, gill openings wide, unconstricted. Eye small but well formed, with distinct lens and covered by thin transparent integument, located dorsally on head, with small lateral component, anterior to middle of HL. Anterior naris round, positioned closer to anterior margin of snout than to anterior margin of eye, surrounded by tube of integument continuous posterolaterally with nasal barbel. Anterior internarial distance slightly less than interorbital. Posterior naris round, smaller than eye, located much closer to eye than to anterior naris, posterolaterally separated from eye by narrow area of soft tissue equivalent to less than half orbital diameter. Short semilunar flap of integument along anterior margin of posterior naris. Posterior internarial distance shorter than anterior internarial distance, approximately 50% of interorbital. Mouth subterminal, wide, upper jaw slightly longer than lower, margin of lower jaw straight or gently convex anteriorly, some specimens with middle portion of lower jaw more convex. Upper lip continuous with remainder of dorsal surface of head and base of maxillary barbel. Lower lip narrow, forming peculiar laterally long narrow lobes well differentiated from remainder of ventral surface of head, nearly meeting at midline. Lobes well separated from base of rictal barbel on each side by integument groove. Integument of both lips smooth under superficial examination, covered with tiny inconspicuous papillae. Premaxillary teeth 17-21, conical, arranged in two irregular rows (7-9 on first row, 10-12 on second one) along nearly entire anterior margin of bone (Fig. 11B). Dentary teeth 20-22, conical, arranged in two rows with equal-sized teeth.

Three pairs of barbels well developed (Fig. 13), with visible internal cores, particularly on maxillary barbel. Base of maxillary barbel broad but continuous with soft portion of barbel, its maximum width less than distance of its posterior margin to eye, internally supported by elongated distal portion of maxilla and less than half as long as soft portion of maxillary barbel. Distance between maxillary barbel bases less broad than head width when protruded. Extended maxillary barbel variably reaching to posterior margin of opercular odontodophore, or to end of pectoral-fin base. Rictal barbel shorter than maxillary barbel, attached to corner of mouth, its base covered dorsally by maxillary-barbel base, variably reaching to end of interopercular odontodophore and beyond margin of branchiostegal membrane when extended. Nasal barbel approximately as long as other barbels, reaching to transverse line through end of opercular odontodophore or slightly short of that. Opercular odontodophore small, round, located immediately anterior to pectoral-fin origin in dorsal projection, surrounded by narrow periodontodal fold (Fig. 13). Eight to ten opercular odontodes (anterior one or two small) clustered in roundish arrangement. Interopercular odontodophore oblong, slightly larger in total area than opercular odontodophore, ventrolateral on head, surrounded by narrow periodontodal fold, slightly produced dorsoposteriorly. Eleven to fourteen interopercular odontodes disposed in two rows.

Lateral line reduced to tiny canal dorsal to pectoral-fin base split in two equaly short branches each opening as terminal pore. Single short and poorly ossified canal bone on upper branch. Sensory canal running through supracleithrum, pterotic and posterior length of sphenotic. Three latero-sensory pores, one at approximately midlength of sphenotic, another at junction sphenotic-pterotic and one at junction pterotic-supracleithrum. Anterior pore (anterior terminus of latero-sensory system) posterior to eye and distant from latter by one-and-a-half eye diameter or slightly less. Frontals lacking sensory canal. Nasal branch (and bone) absent.

Pectoral fin long, narrow, originating immediately posterior to posterior margin of branchial membrane, at vertical through posterior margin of opercular odontodophore (Fig. 13). Pectoral-fin rays I+4 or I+3+I, with last ray variably unbranched, incipiently branched or fully branched. Branched rays splitting once. First pectoral-fin ray (unbranched), markedly longer and thicker than other rays, prolonged as a long filament extending beyond rest of fin by 30-80%. Other rays progressively shorter and thinner, all protruding slightly beyond fin membrane. Pelvic fin small, elongate, its origin posterior to middle of SL, well anterior to vertical through origin of dorsal fin; its posterior end entirely covering anal and urogenital openings, not reaching origin of anal fin in specimens larger than 23 mm SL, and just reaching it in specimens below that size. Pelvic-fin rays I+3+I, all segmented, first and second branched rays longest. Pelvic splint present, extending for approximately basal one-fifth of first segmented ray. Bases of pelvic fins separated by narrow space. Dorsal fin oblong, with round distal margin, its origin on posterior half of SL, anterior to vertical through anal-fin origin and slightly anterior to vertical through end of pelvic fin. Dorsal-fin rays i+II+4+II (5*), i+II+4+I (1), i+III+3+II (1), i+II+5+I (6), first and second branched rays longest, branched rays splitting once. Anal fin oblong, similar in shape and size to dorsal fin, its origin at or slightly posterior to end of pelvic fin, posterior to vertical through origin of dorsal fin. Anal-fin rays i+II+4+I (7*), i+II+3+I (3), i+II+4+II (1, last ray vestigial), all segmented, second branched ray longest, branched rays splitting once. Caudal fin slightly longer than deep, slightly deeper than caudal peduncle when expanded. Caudal-fin margin variable, ranging from gently convex, nearly truncate with round corners to nearly round. Caudal-fin rays 7+6 (1), 5+6 (6*), 6+6 (6), 5+5 (3), or 6+5 (1), all principal rays with similar lengths except slightly shorter upper and lower ones, branched rays splitting once. Procurrent caudal-fin rays nine dorsally and seven to nine ventrally, extending for posterior third or slightly more of caudal peduncle length and merging gradually into principal caudal rays.

Axillary gland evident as tumescent, slightly translucent area posterodorsal to base of pectoral fin in some

specimens, but nearly indistinguishable from remainder of body surface in others. Gland pore small, located anteriorly on gland, axillar in position relative to pectoral-fin base, posteroventral to far more visible pore exiting supracleithrum. Gland pore collapsed as slit in most specimens, filled to surface with coagulated mucus.

Vertebrae 31. First dorsal-fin pterygiophore posterior to neural spine of vertebra 16. First anal-fin pterygiophore aligned with hemal spine of vertebra 17. Ribs three (one CS paratype with additional small supranumerary rib on left side of Weberian complex). Branchiostegal rays six. Seven dorsal- and six anal-fin pterygiophores. Cranial fontanels absent.

Pigmentation in alcohol (Fig. 13): Dorsum and flanks with large irregular, mostly roundish, dark spots, in some specimens arranged in poorly defined longitudinal rows. In most specimens, spots overlain and partly coalesced with additional irregularly-distributed chromatophores obscuring spotted pattern into flaky dusky combined pattern, gradually less dense ventrally to white abdomen. Some specimens with spotted pattern, totally non-obscured by additional pigmentation. Caudal peduncle with same covering as rest of body, with vague outlining of posterior myotomes on posterior region of caudal peduncle. Dorsal surface of head with spots similar yet smaller than those on dorsum, combining with brain pigment over posterior part of braincase. Dark chromatophores concentrated on region between eyes and posterior nares, sometimes spotted and sometimes coalesced in nearly continuous dark covering extending onto dorsal surface of snout and base of maxillary barbels. Small area ventrolateral to eyes lacking dark chromatophores. Dark concentrations on cheeks and dorsal margin of opercular odontodophore. Ventral portion of head mostly white, with few chromatophores on mental region and over interopercular odontodophore. Dorsal surface of pectoral-fin base with concentration of dark chromatophores sometimes forming intense dark spot. Bases of dorsal and anal fins with dark concentration, extending sparsely onto basal part of fin web of former. Pelvic fin hyaline. Base of caudal fin with vertical dark arc crossing bases of principal and accessory rays, along posterior margin of hypural plate, darkest at hypural diastema, forming central dark spot in some specimens. Upper and lower limits of arc extending along limit between last segmented and first accessory caudal-fin rays. Remainder of caudal fin white or with sparse dark markings.

Geographical distribution (Fig. 12): *Salpynx ephebus* is known exclusively from creeks draining the Serra da Mocidade range into the Rio Pacu, itself part of the Rio Branco system, at altitudes around 600 m asl. The locality is the Brazilian State of Roraima, Municipality of Caracaraí.

Ecological notes: According to D.A. Bastos (*pers. comm.*), specimens of *Salpynx ephebus* were collected in a first or second-order terra firme stream, maximally 150 cm in width and 30 cm in depth. Substrate was a mix of fine sand and gravel, covered with fine leaf litter intermingled with root tips. Water was clear, cool (20-23°C), acidic (5.1-5.7 pH) and with moderate current. Fish were found hiding among roots and sand and were collected by hand seining against banks. The species was restricted to the altitude range around 600 m asl. Additional collecting both at lower altitudes and higher (800-1,000 m asl) in the same stream and seemingly similar habitat failed to secure any specimens. In the upper range (800-1,000 m), a species of *Trichomycterus* related to *T. guianensis* is abundant, but none was found in the *S. ephebus* range (600 m). Only three other species were found to co-occur with *S. ephebus,* namely *Ancistrus* sp. (Loricariidae), *Bryconamericus* sp. (Stevardiidae), and *Erythrinus erythrinus* (Erythrinidae).

Etymology: Latinized Greek word ephebus refers to ephebos, a youth in ancient Greece. This is an allusion to the name of the mountain range where the species was found, Serra da Mocidade, meaning "range of youth" in Portuguese. A noun in apposition.

Monophyly of *Salpynx:* The articulation of the cleithrum with the skull in trichomycterids is formed by a roundish space framed by the epioccipital and a narrow bony loop of the supracleithrum anteriorly, with the dorsal tip of the cleithral process fitting within that orifice and visible in dorsal view. This is a widespread condition in trichomycterids, including most glanapterygines (in *Glanapteryx* the orifice is closed by overlaying secondary ossification). Species of *Salpynx,* however, share an independent and hypertrophied fenestra anterior to that orifice, framed by the pterotic and epioccipital anteromesially, the supracleithrum laterally and the margin of the Weberian capsule posteromesially (Fig. 1-3, SF). The fenestra thus formed, which we call a supratemporal fenestra, is a prominent feature of the skull roof and several times larger than the adjacent cleithral orifice. It seems to have a purely structural function and does not serve as passage either for nerves or blood vessels or for muscle insertion. A far less prominent situation is seen in *Hyaloglanis, Pygidianops* and *Typhlobelus* species and some *Listrura* (*e.g., L. tetraradiata*). It is possible that the less extreme condition is synapomorphic for a broader clade, but intermediate conditions make it difficult at this time to delimit clear-cut states and their phylogenetic significance. The only situation similar to that in *Salpynx* is seen in the Trichomycterinae (cf. Chardon, 1968, figs. 164, 167; Reis *et al.,* 2019, fig. 5), a condition verified in representatives of all genera except *Rhizosomichthys.* We consider the fenestra in *Salpynx* and trichomycterinaes to be homoplastic due to the presumed phylogenetic distance between the two taxa (Reis *et al.,* in press). If that is the case, then the fenestra is not only a synapomorphy for *Salpynx* but also an additional synapomorphy for the Trichomycterinae. There are minor structural differences between the fenestra in the two taxa, with the one in *Salpynx* having well-defined margins all around and its entire perimeter on the same plane. The one in Trichomycterinae has more heterogeneous margins, with its various components on different planes, looking more like a leftover space left in

the conjoining of the Weberian capsule to the back of the skull rather than a dedicated fenestra. The situation in Trichogeninae and Copionodontinae is difficult to compare because of their radically different configurations of the occipital region, shoulder suspension and swimbladder capsule, where the latter is well separated from the back of the skull. It of course possible that the space of the fenestra is a leftover from the incomplete conjoining of the Weberian capsule to the back of the skull, and thus plesiomorphic. In any case, the well-defined rim of the fenestra in *Salpynx* is an apomorphic modification on the circumscribed space, thus apomorphic. Ontogenetic data will be necessary to resolve the question in more detail.

The barbular bone in all species of *Salpynx* is short (slightly over 50% of the longest axis of the palatine exclusive of the posterolateral process), stout and peculiarly expanded and bilobed at its posterior end (Fig. 1-4). This set of modifications is highly divergent from the widespread condition of the bone in all other trichomycterids where it is present (several subsets of the family entirely lack the barbular, most notably the Tridentinae, Stegophilinae, and Vandelliinae). In the widespread and putatively plesiomorphic condition, the barbular is long (approximately as long as the longest axis of the palatine exclusive of the posterolateral process), thin, with fine anterior and posterior ends. Some trichomycterins exhibit a lateral expansion or bifurcation in the barbular (*e.g., Trichomycterus alternatus, T. astromycterus; Ituglanis* sp.). However, this modification differs from that of *Salpynx* in being located at the midportion of the bone rather than at its posterior end. Moreover, the trichomycterins that exhibit this feature are phylogenetically distant from *Salpynx* (Reis, 2023). Most species of *Hyaloglanis* have a vestigial barbular (in the form of a miniscule blob of bone) or lack the bone entirely. However, *H. nheengatu* has a well-developed short barbular, thickened posteriorly and closely adpressed to the skull (Canto *et al.,* 2022, fig. 2). The bone differs from that in *Salpynx* in not being bilobed posteriorly. *Hyaloglanis nheengatu* may be the sister species to the rest of the genus, given its comparatively smaller cranial fontanel, and the presence of a well-developed barbular. If so, the stout barbular may provide circumstantial evidence for a group composed of *Salpynx* + *Hyaloglanis,* with the bilobed condition being exclusive to *Salpynx*.

***Hyaloglanis,* new genus**

https://zoobank.org/FD6F5BA0-23DF-4C00-88FF-36BB01519B42

Type species: *Ammoglanis pulex* de Pinna & Winemiller, 2000.

Diagnosis: The genus can be uniquely diagnosed by: (1) a scythe-shaped lacrimal-antorbital (Fig. 5) and (2) the presence of dark pigmentation in the sagittal plane of the body (visible in life on both sides of the body due to transparency) (Fig. 7). Other characteristics not unique to *Hyaloglanis* yet diagnostic across large subsets of Trichomycteridae include: (1) absence of metapterygoid (also in *Glanapteryx, Tridens,* and *Tridensimilis*); (2) absence of a cartilaginous tip at the dorsal end of the ascending process of the quadrate (also in *Glanapteryx, Pareiodon, Tridens,* and *Tridensimilis*) (Fig. 14). Further distinguished from *Salpynx* by the wide-open cranial fontanel, which leaves most of the central part of the skull roof unossified (Fig. 5, *vs.* skull roof entirely ossified, lacking fontanels), by the vomer broader than long (*vs.* vomer elongate); by the ventral process of the maxilla laterally directed (Fig. 5).

Etymology: From the Greek hyalos-, transparent, and -glanis, catfish, in allusion to the translucent aspect in life of the species included in the genus.

Species included: *Hyaloglanis natgeorum* (Henschel, Lujan & Baskin, 2020); *H. nheengatu* (Canto, Hercos & Ribeiro, 2022); *H. obliquus* (Henschel, Bragança, Rangel-Pereira & Costa, 2020), and *H. pulex* (de Pinna & Winemiller, 2000).

Monophyly of *Hyaloglanis:* A peculiar scythe-shaped lacrimal-antorbital with an anterior articuar facet for the palatine cartilage was originally proposed as an autapo-

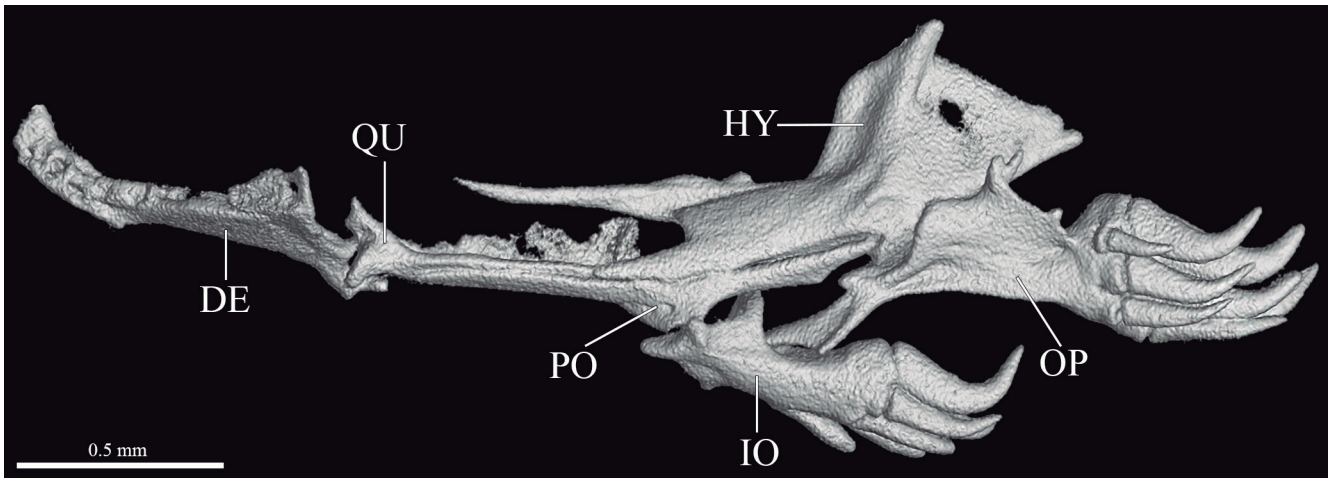

Figure 14. *Hyaloglanis pulex,* MZUSP 42471, CT-scan images of suspensorium in lateral view. Scale bar = 0.5 mm. Abbreviations: DE, dentary; HY, hyomandibular; IO, interopercle; OP, opercle; PO, preopercle; QU, quadrate.

morphy for *H. pulex* by de Pinna & Winemiller (2000). The condition is peculiar in that the bone is elongate, with a relatively simplified and continuous surface, a broad longitudinal groove along most of its length and narrowing markedly to a fine posterior tip, which is curved mesially (Fig. 5). This contrasts with the lacrimal normally seen in a majority of other trichomycterids, which has a rather irregular surface, with a posterior tip which is blunt (although usually narrower than the anterior portion) and not markedly curved. The same scythe-shaped condition of the lacrimal is reported for all other species herein included in *Hyaloglanis,* (*H. natgeorum, H. obliquus,* and *H. nheengatu;* cf. Henschel *et al.,* 2020a, b; and Canto *et al.,* 2022). The condition has also been reported for *S. amapaensis,* but that does not seem to agree with the illustration provided in Mattos *et al.* (2008, fig. 5) which shows a lacrimal lacking the two main traits which identify the condition, the pronounced posterior narrowing to a fine tip and the mesial posterior curvature. In *S. amapaensis* the posterior end of the lacrimal is blunt and the curvature is outward (*i.e.,* lateral margin concave, mesial margin convex) or the bone is approximately straight (Mattos *et al.,* 2008, fig. 5). It is possible that there are some special elements in the lacrimal-antorbital morphology shared in species of *Hyaloglanis* and *Salpynx* or perhaps even larger assemblages. Some parts of the scythe morphology may be present in *S. trombetensis* and *S. ephebus, Malacoglanis gelatinosus* and *Sarcoglanis simplex*. Such anatomical subtelties may hold valuable information at more inclusive levels. However, sorting out this diversity will require a detailed comparative study of the lacrimal-antorbital which extrapolates the present work. At this time, the nearly identical condition in species of *Hyaloglanis* can be considered with certainty as unique to that clade. Some interesting previously unreported situation was observed in *H. obliquus,* where the posterior tip of the lacrimal is prolonged into a long, curved (continuing the arc of the scythe-shaped lacrimal), extremely thin thread-like ossification extending to near the margin of the skull and terminating in a tiny nodule. That nodule is apparently a reduced barbular, having the same position and shape as the presumed barbular (labeled as antorbital) reported in de Pinna & Winemiller (2000, fig. 6) for *H. pulex*. The situation in the latter species is actually similar to that in *H. obliquus,* but with the curved ligament unossified or very poorly ossified. The whole structure seems to be an ossification of the fronto-lacrimal tendon, but its curved shape and ossification continuous with the lacrimal (at least in *H. obliquus*) are unique, and its homology to the barbular of more generalized trichomycterids is restricted to the terminal nodule. More information on other species of *Hyaloglanis* is necessary to ascertain its phylogenetic significance.

An unusual internal pigmentation pattern was first described for *Hyaloglanis pulex* (de Pinna & Winemiller, 2000). The species has internal (nondermal) dark chromatophores on the sagittal plane of the body that form a pattern of seven to nine vertical bands seen from both sides of the fish due to transparency in life (Fig. 7). The internal chromatophores are apparently distributed on the sagittal intervertebral septum, also known as the vertical septum. The banded pattern formed by such nondermal chromatophores is reinforced by matching integumentary (dermal) chromatophores on dorsum, but not on the sides. The result is a compound banded pattern where the lateral aspect is formed by nondermal sagittal chromatophores seen by transparency and the dorsal aspect by normal dermal chromatophores (Fig. 7). Post-mortem opacity prevents visibility of most of the lateral nondermal bands in preserved specimens, except for sometimes the posterior one or two in the caudal peduncle (Fig. 15). The banded pattern remains visible dorsally in preservation due to its integumentary chromatophores. The pattern of internal pigmentation forming bands visible on both sides by transparency is common to all species of *Hyaloglanis* (de Pinna & Winemiller, 2000; Henschel *et al.,* 2020a, b; and Canto *et al.,* 2022). This condition is otherwise unique among trichomycterids and a synapomorphy for the genus. Dissection of alcohol-preserved paratypes of *Salpynx ephebus, S. ix* and *S. trombetensis* revealed internal chromatophores along vertebrae, distributed in irregular streaks not forming any specific pattern, and none on the sagittal plane. The same condition seems to apply to photos of live specimens of *S. amapaensis* (Fig. 6). In *Ammoglanis diaphanus* there are only few internal chromatophores dotted along the vertebrae in cleared but not bleached specimens. The only other trichomycterids documented with a degree of soft tissues transparency in life similar or superior to that in species of *Hyaloglanis* are *Tridens* spp. (cf. Henschel *et al.,* 2023, fig. 14 for the condition in *T. chicomendesi*) and *Stauroglanis goudingi*. In the former, internal chromatophores are apparently present as dots along the dorsal part of the gut, along the radials and anterior distal part of anal-fin pterygiophores and posterior dorsal part of caudal vertebrae. *Stauroglanis goudingi* has internal dark chromatophores along the vertebral column, forming a longitudinal row of elongate spots along the center of the body visible externally in the live fish (Zuanon & Sazima, 2004, fig. 1), with chromatophores restricted to the tissues immediately around the vertebral column and not extending on the sagittal plane, in contrast to *Hyaloglanis.* A similar situation is seen also in species of *Microcambeva* (cf. Costa & Katz, 2021, fig. 6) and of *Homodiaetus* spp., where internal dark chromatophores along the vertebral column are visible externally as a regular dashed pattern, but not extending on the sagittal plane. Outside of siluriforms, a parallel chromatic strategy is apparent in at least one species of *Microschemobrycon,* (*M. cryptogrammus* Ohara *et al.,* 2019) where a continuous dark lateral band is evident along the entire length of live specimens, mostly composed of internal chromatophores along the vertebral column. After fixation, it is evident that only the extreme anterior and posterior ends of the band is expressed in external chromatophores (Ohara *et al.,* 2019, cf. figs. 1 and 2), all the rest being internal pigment seen by transparency. Nondermal, internal pigmentation in fishes has not been extensively studied and its adaptive role is controversial and probably multiple (Nilsson-Sköld

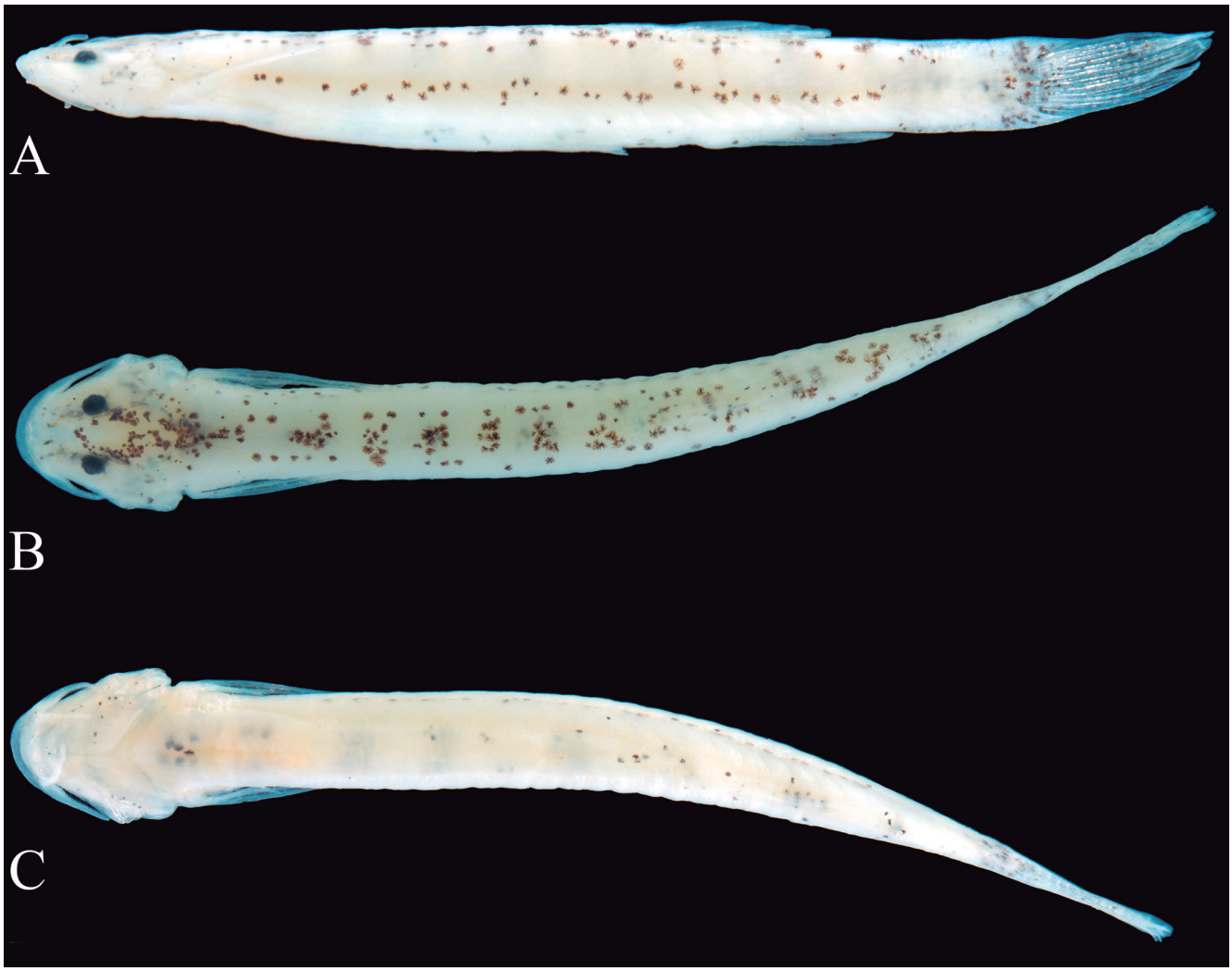

Figure 15. *Hyaloglanis pulex,* IAvH-P 15986, (A) lateral view; (B) dorsal view; (C) ventral view. Photographs by Jorge E. García-Melo.

et al., 2016). It has been demonstrated that internal chromatophores in the peritoneum and around the skeleton can be responsive to the background by pigment translocations melanocytes in the ice goby, *Leucopsarion petersii* (Goda & Fujii, 1996). Internal chromatophores also react to re-exposure to melatonin and norepinephrine just like superficial chromatophores and such response is more pronounced in transparent fish (Nilsson-Sköld *et al.,* 2010). This suggests that in transparent fish the role of internal chromatophores is similar to that of integumentary chromatophores, *i.e.,* to interact chromatically with external factors (camouflage, mimicry, intra- and interspecific signaling etc.). Species of *Hyaloglanis* probably fit this pattern, with the added peculiarity of having their overall body coloration of well-defined banded pattern resulting from an integration of dermal (dorsal view) and nondermal (lateral view) chromatophores. Internal pigmentation is particularly conspicuous in larval fishes, which tend to be highly transparent (cf. Baldwin, 2013). Being such small fishes, the question arises whether the internal pigmentation condition in *Hyaloglanis* is paedomorphic or an entirely new adult condition. At this time, there is not enough information on larval forms of possibly related forms to address this issue.

A key to species of *Salpynx* and *Hyaloglanis*

The aim of this key is practical and as much as possible emphasizes traits of external morphology easily accessible in intact alcoholic specimens. Such traits are thus listed first in each doublet. Characters of internal anatomy and more laborious to verify are included as complements for cases where additional confirmation may be needed. Data for species not directly examined were obtained from original descriptions.

1. Pelvic fins covering anal opening, their margin nearly reaching origin of anal fin (Figs. 6, 9, 10, 13); mental region lacking finger-like papillae (or barbelets); eyes widely separated (interorbitalequivalent to 3.5-4.5 eye diameters; Figs. 9, 13); body darkly-pigmented, predominantly brown due entirely to superficial integumentary chromatophores (Figs. 6, 9, 10, 13); skull roof entirely closed, lacking cranial fontanels (Figs. 1, 2, 3)..... 3 (*Salpynx*)
2. Pelvic fins not covering anal opening, their margin distant at least their own length from origin of anal fin (Fig. 15); mental region with pair of finger-like papillae (or barbelets); eyes close together (interorbital equivalent to 2-2.5 eye diameters; Fig. 15); body lightly pigmented, predominantly white (translucent in life), with pattern of vertical bars disposed along entire body, formed by combination of superficial

integumentary chromatophores plus internal dark chromatophores on the sagittal plane, fully visible in live fish only (Fig. 7), only partially observable in preserved specimens (Fig. 14); skull roof mostly uncovered by bone, as single large fontanel (Fig. 5) ..... 6 (*Hyaloglanis*)

3.1. Premaxillary teeth in two regular or irregular rows (Fig. 11A, B); ribs three 4

3.2. Premaxillary teeth in one row (Fig. 11C); ribs two 5

4.1. Premaxillary teeth 32-37, arranged in two rigidly regular rows (Fig. 11A); dentary teeth 33-34, disposed in three regular wavy rows (with anterior row short, near symphysis only) and teeth gradually larger towards symphysis in each row; sensory canal running through nearly entire length of sphenotic (Fig. 1) ..... *S. trombetensis*

4.2. Premaxillary teeth 17-21 arranged in two irregular rows (Fig. 11B); dentary teeth 20-22, disposed in two rows, with similar-sized teeth along each row; sensory canal running through posterior half, or slightly more, of sphenotic (Figs. 2, 3)..... *S. ephebus*

5.1. Dentary teeth 12 to 15; anterior palatine ossification absent..... *S. ix*

5.2. Dentary teeth 7 or 8; anterior palatine ossification present ... *S. amapaensis*

6.1. Jaws totally edentulous, lacking both premaxillary and dentary teeth (Fig. 5, 14); four pelvic-fin rays..... *H. pulex*

6.2. Upper jaw with some small conical teeth on both premaxilla and dentary; five pelvic-fin rays 7

7.1. Eight or ten premaxillary teeth; pelvic splint present; barbular bone present and well developed; single cranial fontanel a large lozenge occupying central portion of braincase ..... *H. nheengatu*

7.2. Seven or fewer premaxillary teeth; pelvic splint absent; barbular bone absent or vestigial; single cranial fontanel occupying entire dorsal surface of braincase, leaving practically no bony skull roof..... 8

8.1. Four to six premaxillary teeth; eight or nine dentary teeth; five pectoral-fin rays; vertebrae 31..... *H. natgeorum*

8.2. Three premaxillary teeth; four dentary teeth; six pectoral-fin rays; vertebrae 34-35..... *H. obliquus*

DISCUSSION

The original description of the genus *Ammoglanis,* then with a single species *A. diaphanus* (Costa, 1994) lists four synapomorphies for the genus: (1) a slender quadrate, its greatest depth 30% of the length of its main axis; (2) an expanded anterior tip of interopercle, about 50% of the total length of the upper margin of this bone; (3) premaxilla posterior to mesethmoid cornu; (4) ventral mouth. The four characters are unusual and clearly apomorphic. However, species subsequently described and included in *Ammoglanis* have shared only the first of those. Henschel *et al.* (2020a) noticed this fact, expanding the definition of that first character to a range covering a quadrate depth of 15-30% of its length. Concomitantly, Henschel *et al.* (2020b) added a total quadrate length of 75% of the length of the hyomandibula as a further qualification of the character. Clearly, the clear-cut condition originally described for *A. diaphanus* has become gradually less well-defined as additional species with intermediate conditions were added to the genus. At this time, the shape of the quadrate is quite evidently a difficult to quantify set of proportions which on the whole do not provide well-defined states for the various taxa as was the case in *A. diaphanus* only. In the end, those additional taxa were included in *Ammoglanis* on relatively weak evidence, coupled with a lack of evidence for better alternatives. The species herein moved to *Salpynx* and *Hyaloglanis* do not share any of the characters originally given as apomorphic to *A. diaphanus,* which at the moment are likely autapomorphic for that species. The discussion below thus focuses on a broader range of comparisons in trying to elucidate relationships beyond the confines of *Ammoglanis.*

Relationships of *Salpynx* and *Hyaloglanis* with Glanapteryginae

Evidence for an alignment of *Salpynx* and *Hyaloglanis* with Glanapteryginae comes from three different anatomical complexes, palatine, latero-sensory canal system and pectoral girdle, each treated in separate subsections below.

Palatine (Fig. 1-5): The structure of the palatine provides the most visible piece of evidence for the placement of *Salpynx* and *Hyaloglanis* in Glanaptegyginae and in fact for diagnosing the entire subfamily. That single bone serves as a decisive proxy for the separation of sarcoglanidines from glanapterygines in their traditional senses (*i.e.,* exclusive of *Listrura* in Microcambevinae), so far with no exceptions or intermediate character conditions. First, in both *Salpynx* and *Hyaloglanis* the palatine lacks a significant portion posterior to the articulation with the neurocranium. In a majority of other taxa in Trichomycteridae the palatine has a posterolateral process that extends posteriorly far beyond that articulation, lending the palatine a very different general shape, with a significant posterior portion. The latter condition is inferred to be plesiomorphic for trichomycterids and is seen in a particularly clear form in sarcoglanidines, including the type species of *Ammoglanis, A. diaphanus* and its now only congener *A. multidentatus* (Fig. 16). The species *H. pulex, H. obliquus, H. natgeorum,* and *H. nheengatu,* all previously in *Ammoglanis,* have the short version of the palatine (Fig. 5) typical of glanapterygines, rather than the long state as in *A. diaphanus.* The same applies to all species herein included in *Salpynx.* Second, the posterolateral process of the palatine in both *Salpynx* and *Hyaloglanis* is broadly triangular and strongly deflected laterally, oriented at approximately right angle relative to the lateral margin of the bone (Fig. 1-5). This is the same situation seen in all glanapterygines with an identifiable homologous process, but in no sarcoglanidines or other trichomycterids. The condition was noticed as a state shared between *H. pulex* and *S. amapaensis* in contrast to *A. diaphanus* by Mattos *et al.* (2008) and Costa *et al.* (2019b), a similarity later expanded to *H. obliquus* by Henschel *et al.* (2020a) and to *H. natgeorum* by Henschel *et al.* (2020b). Third, the articulation of the palatine with the skull in all Glanapteryginae including *Salpynx* and *Hyaloglanis* is mediated by a single, posteriorly-oriented, articular facet with the lateral ethmoid (Fig. 4). The palatine suspension thus hinges on a single rather small posterior articulation with the lateral ethmoid. A vestige of an anterior facet remains in some taxa, indicating that the main articulation remaining is the

primitive one with the lateral ethmoid, rather than a conjoining of the two original articulations. In all Sarcoglanidinae, including *A. diaphanus* and *A. multidentatus,* the palatine has two well-defined articulations with the skull, an anterior one with the vomer and a posterior one with the lateral ethmoid, a configuration widespread in "lower" trichomycterids (Fig. 16). There are a few modifications of those patterns. For example, in *Malacoglanis* the palatine has a single and very long articulation with the lateral ethmoid, a situation unique to that genus and likely autapomorphic. *Sarcoglanis* has an apparently intermediate condition where the two articulations are expanded and nearly continuous, both with a mostly lateral plane of articulation. In Tridentinae, the articulation is quite distant in the ossified parts, but clearly there is a soft tissue connection with the vomer and another with the lateral ethmoid. The Vandelliinae, which lack a vomer, have a palatine with a unique stalk-like process articulating laterally with the lateral ethmoid, again a synapomorphic state for the subfamily and not comparable with the one in glanapterygines. In *Potamoglanis* there is a largely continuous long articulation hinging both on the lateral ethmoid and the vomer, with a predominantly lateral component with the former and posterior with the latter. The situations of the palatine suspension in all those taxa are fundamentally distinct from that in *Salpynx, Hyaloglanis* and glanapterygines, which are therefore considered as homologous and putatively synapomorphic. In sum, the set of palatine modifications provide a minimum of three characters aligning *Salpynx* and *Hyaloglanis* with the Glanapteryginae, but excluding *Ammoglanis diaphanus* and *A. multidentatus.* Such discrepancy in palatine morphology has been noticed in Costa *et al.* (2019b: 66), and considered as evidence of proximity between *H. pulex* and *S. amapaensis* (then both in *Ammoglanis*) relative to *A. diaphanus* and *A. multidentatus.*

Laterosensory canals: The Trichomycteridae display various reductions of the latero-sensory canal system (Arratia & Huaquin, 1995; Rizzato & Bichuette, 2016; Pastana *et al.,* 2019). The Glanapteryginae s.l. include some of the most extreme reductions of latero-sensory canals in siluriforms, with variations of degree among different component taxa. In no case the canal enters the frontals or beyond, meaning that the supraorbital and nasal branches are absent in all glanapterygines. The least reduced version is seen in species of *Glanapteryx,* where the canal is present in the pterotic and extends into the sphenotic all the way to its anterior end. The situation is variable in *Pygidianops,* with some species having the canal extending to the posterior half of the sphenotic (*e.g., P. cuao*) and others restricted to the pterotic (*e.g., P. amphioxus*). In *Listrura,* the canal is restricted to the pterotic, except in *L. tetraradiata* where it extends to the middle of the sphenotic. Species of *Typhlobelus* have the canal restricted to the pterotic, with at least one species, *T. auriculatus,* having no actual canal anywhere in the skull. Exactly the same reductions are seen in species of *Salpynx* and *Hyaloglanis.* In *Salpynx* species, the canal extends anteriorly to approximately half the length of the sphenotic in all three species, a condition evident externally by the superficial pores (Fig. 8). A more extreme reduction occurs in species of *Hyaloglanis,* where there is no complete latero-sensory canal anywhere beyond the

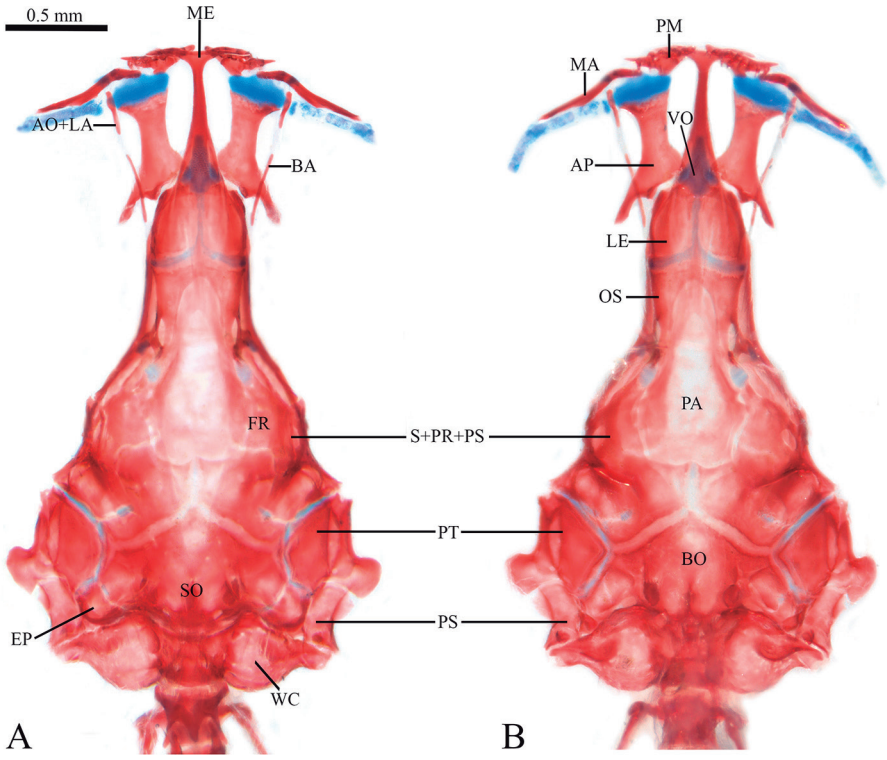

Figure 16. *Ammoglanis diaphanus,* MZUSP 86249, CS specimen, head, (A) dorsal view, (B) ventral view. Scale bar = 0.5 mm. Abbreviations: AP, palatine; AO+LA, lacrimal-antorbital; BA, barbular; BO, basioccipital; EP, epioccipital; FR, frontal; LE, lateral ethmoid; MA, maxilla; ME, mesethmoid; OS, orbitosphenoid; PA, parasphenoid; PM, premaxilla; PT, pterotic; PS, supracleithrum; S+PR+PS, sphenotic-prootic-pterosphenoid; SO, supraoccipital; VO, vomer; WC, Weberian capsule.

supracleithrum. Their pterotic has a small vestigial canal laterally only, keeping a sensory pore corresponding to the pterotic branch. In any event, such reductions of the latero-sensory canal system in the skull are unique to glanapterygines (the closest condition is in the trichomycterine *Silvinichthys,* but here the nasal portion of the canal is retained anteriorly) and provide strong evidence of their relationships with *Salpynx* and *Hyaloglanis.* No other trichomycterids, including no sarcoglanidines, have a similar situation. While most likely related to some form of paedomorphosis, such reductions of sensory canals are not paralleled in other miniature trichomycterids. For example, *Ammoglanis diaphanus* and *Potamoglanis* spp., some of the small species of *Paracanthopoma* and Tridentinae have body sizes overlapping with those of the smallest glanapterygines, yet all of them have sensory canals extending continuously from the supracleithrum into the frontal. This is the case even in taxa with extremely reduced frontals, where the corresponding supraorbital canal runs through soft tissue adjacent to the margin of the remaining frontal ossification, as in some tridentines (Pastana *et al.,* 2019; de Pinna *et al.,* 2024). So, the reduced condition in Glanapteryginae (including *Salpynx* and *Hyaloglanis*) is unique. Despite some variation in the degree of canal reduction among different glanapterygine taxa, the common reduced condition is considered as a single objective character.

Pectoral girdle: Interesting modifications of the pectoral-fin supports are shared between *Salpynx, Hyaloglanis,* and other members of the Glanapteryginae. Their proximal pectoral-fin radial (the single element of the series in trichomycterids) is an attenuated form of the pronounced fan-shape in most trichomycterids, only gently expanded at the distal end (Fig. 17), or shaped either like a cylinder, or as a dumbbell with mildly and symmetrically expanded ends. This contrasts sharply with the situation of that bone in other trichomycterids, including all sarcoglanidines, where the proximal and distal ends are highly asymmetrical in width, with the latter dramatically expanded, strongly fan-shaped. Because the distal

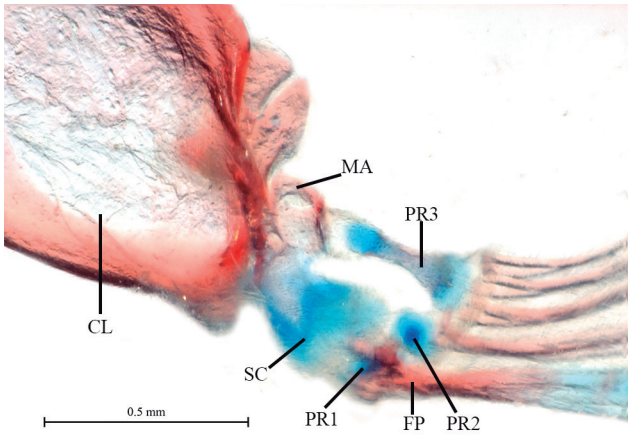

Figure 17. Pectoral girdle of *Salpynx trombetensis* **sp. nov.**, paratype, MZUSP 130303, left side, ventral mesial view. Abbreviations: CL, cleithrum; MA, mesocoracoid arch; FP, first pectoral-fin ray; PR1-3, proximal radial 1 to 3; SC, scapulocoracoid.

end of the radial is responsible for the support of most fin rays, one would expect that its reduction would be associated with an equivalent reduction of fin-ray number, as is the case in many glanapterygines. Nonetheless, the radial attenuation is present in taxa with comparatively well-developed fin rays, such as species of *Salpynx* and *Hyaloglanis,* and *Listrura tetraradiata.* Both *Ammoglanis diaphanus* and *A. multidentatus* retain the plesiomorphic condition of the pectoral-fin ray supports.

Immediately anterior to the proximal radial discussed above is the scapulocoracoid, which in most trichomycterids (Copionodontinae and Trichogeninae being exceptions) is reduced to a short complex bone attached to the posterolateral surface of the cleithrum and closely involved in the suspension of the first pectoral-fin ray. In glanapterygines, including *Salpynx* and *Hyaloglanis,* the scapulocoracoid is modified into a protruding and partially mobile elongate structure, often mostly cartilaginous, articulating distally with the first pectoral-fin ray and biomechanically acting almost like an extra radial. This is an apomorphic condition for the clade and the only parallel occurrence is in vandelliines. The latter share a common ancestor first with Stegophilinae and second with Tridentinae, both clades with plesiomorphic scapulocoracoids, and are therefore phylogenetically distant any possible common ancestor with glanapterygines (de Pinna, 1998; DoNascimiento, 2015; Ochoa *et al.,* 2020; Reis, 2023). Thus, the condition of the scapulocoracoid in vandelliines is interpreted as convergent. The set of modifications in the pectoral-fin support in glanapterygines, *Salpynx,* and *Hyaloglanis* described above comprise minimally two characters: the attenuated proximal pectoral-fin radial and the mobile rod-like scapulocoracoid.

Possible monophyly of *Salpynx* plus *Hyaloglanis*

A recent phylogenetic analysis with a selected range of trichomycterids and employing a variety of morphological, molecular and total-evidence analyses (Reis *et al.,* in press) included *Salpynx ix* and *Hyaloglanis pulex* as terminals (treated in their original genera, *Stenolicmus* and *Ammoglanis,* respectively). Despite variation in hypothesized relationships in parts of the different trees found, the two later taxa were invariably recovered as sister groups. The evidence for that was exclusively morphological, as sequence data is yet unavailable for both and in combined analyses their corresponding molecular partition was treated as missing. Despite that, none of the evidence bringing the representatives of *Salpynx* and *Hyaloglanis* together is unique. The most convincing evidence for that relationship lies in the structure of their lateral ethmoids. In all species of both *Salpynx* and *Hyaloglanis,* the lateral ethmoids in dorsal and ventral views are narrow bones separated by a wide median space. Also, each bone is curved mesially, so that only their anterior ends are in contact or in close proximity, bracing almost directly on each side the posterior end of the ethmoid cartilage medially (Figs. 3-5). This set of modifications (which might arguably be considered as separate characters) is striking in a gen-

eral view of the skull, and evident in published illustrations of some of the species which we could not examine directly (such as *H. nheengatu;* cf. Canto *et al.,* 2022, fig. 2). In the plesiomorphic condition, the lateral ethmoids are relatively wide bones in contact or close proximity for their entire mesial margin, a state observed in the majority of other trichomycterids, including *Ammoglanis diaphanus, A. multidentatus* and other sarcoglanidines (Fig. 16). The condition, however, is not exclusive to *Salpynx* and *Hyaloglanis.* Species of *Potamoglanis* also have widely separated lateral ethmoids converging anteriorly. Their situation differs in detail from that in *Salpynx* and *Hyaloglanis,* because their contact with the ethmoid cartilage is wider, with a large anterior component, with the bracing not as directly mesial as in *Salpynx* and *Hyaloglanis.* Still, such differences are not enough to reject primary homology. Current competing hypotheses about the phylogenetic position of *Potamoglanis* include its position as sister group to *Sarcoglanis* (Ochoa *et al.,* 2017), as sister group to Sarcoglanidinae plus *Pygidianops* and *Typhlobelus* (Ochoa *et al.,* 2020), and as sister group to Tridentinae (Henschel *et al.,* 2017). To those hypotheses, Reis *et al.* (in press) recently added the possibilities of *Potamoglanis* as sister group to Glanapteryginae s.l., or as sister group to the TSV clade, or to the group composed of Glanapteryginae (including *Salpynx* and *Hyaloglanis*) plus the TSV clade. In sum, the position of *Potamoglanis* remains basically unresolved at that level. *Potamoglanis* does not share the various putative synapomorphies that *Salpynx* and *Hyaloglanis* share with Glanapteryginae (see above).

In association with the previous character, the parasphenoid in *Salpynx* and *Hyaloglanis* occupies the space between the lateral ethmoids, forming the floor of the neurocranium also along the ethmoid region (Figs. 1-5). Accordingly, the anterior portion of the parasphenoid is broad and extends medially almost to the anterior end of the lateral ethmoids. In other trichomycterids the parasphenoid is anteriorly narrow and either does not reach the area of the lateral ethmoids or, when it does, simply overlaps their median articulation. This is a widespread condition in other siluriforms as well. A configuration similar to that in *Salpynx* and *Hyaloglanis* occurs in Tridentinae and *Potamoglanis,* where the parasphenoid also occupies the space left between the lateral ethmoids. There are differences of detail in the mode of contact and delineation of the parasphenoid and lateral ethmoid among the different taxa, but not sufficient to refute primary homology. While the condition in tridentines can be hypothesized as convergent based on phylogenetic distance, uncertainties regarding the phylogenetic position of *Potamoglanis* discussed above impede a conclusive resolution of the significance of this character at the moment.

In sum, a sister group relationship of *Salpynx* and *Hyaloglanis* seems the best corroborated hypothesis at this time, but one which still requires further testing by inclusion of additional species of both genera in a broad phylogenetic analysis, as well as a search for additional unambiguous characters and, of course, sequence data for a majority of the taxa concerned.

Ammoglanis multidentatus is an interesting species. While it certainly does not share the synapomorphic conditions for either *Salpynx, Hyaloglanis* or Glanapteryginae s.l. Most evidently, its palatine morphology does not fit the one typical of the Glanapteryginae s.l. (including *Salpynx* and *Hyaloglanis*), bearing instead a long posterolateral process and a double articulation with the skull. *Ammoglanis multidentatus* has a striking ascending process attached to the dorsal surface of the posterolateral process of the palatine, a structure otherwise seen only in species of *Listrura*. This latter process is discussed in Costa *et al.* (2019b) and proposed as a unique trait of *Ammoglanis multidentatus,* although curiously identified as a ventral process of the barbular bone rather than as a dorsal process of the palatine. In our single skeletal preparation of the species (UNT 10003), the process is clearly attached to the palatine. We have not examined their specimen so cannot explain the discrepancy. The evidence aligning *A. multidentatus* with *A. diaphanus* is limited, basically the admittedly nebulous elongate slender quadrate (see above). Still, at this time inclusion of *A. multidentatus* in *Ammoglanis* is the best possible placement. Relationships of the two species now in *Ammoglanis,* both to each other and to other trichomycterids, still need further investigation.

Biogeography

The geographical distribution of *Salpynx* and *Hyaloglanis,* as well as that of the putative clade including the two genera, matches some well-defined biogeographical patterns identified for Amazonian fishes (Dagosta & de Pinna, 2019). The combined distributions of *Salpynx* plus *Hyaloglanis* fits a broad pattern called Eastern Amazon/East of the Purus Arch (Dagosta & de Pinna, 2019: 26), which comprises distributions variably spanning the Orinoco, Negro, Essequibo and Amazonian versants of the Guyanan and Brazilian Shields (including the Madeira, Tapajós and Tocantins/Araguaia) but excluding northeastern Atlantic Guiana Shield drainages. The genus *Salpynx,* in turn, is restricted to rivers draining the Amazonian versant of the Guyana Shield, with the apparently outlier occurrence of *S. ephebus* (Fig. 12) being on the presumably relictual shield outcrop of Serra da Mocidade (Reis *et al.,* 2021). Species of *Hyaloglanis* follow a relatively rarefied series of occurences following the Central Blackwater pattern (Dagosta & de Pinna, 2019: 41), a pattern which is not literally restricted to blackwater rivers. The distribution of the genus matches almost perfectly some of the species previously identified in that pattern, such as that of the cichlid genus *Dicrossus* (Dagosta & de Pinna, 2019, fig. 22C). The abundant repetitive cases supporting the Central Blackwater pattern are indicative of strong historical connections among the rio Negro, Madeira and Tapajós, although one which does not have a consensual historical explanation as yet (Dagosta & de Pinna, 2019).

Current sampling of species of *Salpynx* and *Hyaloglanis* is expected to be incomplete, given their small size and ecology, as well as the fact that some of them have been

sampled but once to date. Also, parts of their areas of occurrence are still incompletely sampled in general, such as the Amazonian versants of the Guyana Shield. Based on the patterns recognized above, a few predictions can be made about new records to be expected (or not expected) for these taxa. Guyanan shield *Salpynx* are expected to occur also in yet poorly-sampled basins which are normally part of that pattern, such as the Uatumã and Urubu. The provenance of *S. ephebus* suggests that additional representatives of the genus may be expected in relictual massifs of the Guyana Shield within the Amazonian versant. It is highly probable that representatives of *Hyaloglanis* will eventually be found throughout the Rio Negro, a major distributional gap in their range in the Central Blackwater Amazon. Likewise, their presence in the Madeira and Trombetas is also likely. The latter drainage is actually an area of partial overlap between the Central Blackwater and Eastern Amazon patterns.

Probable less-than-obvious distributional absences can also be inferred on the basis of the general patterns. For example, representatives of both *Salpynx* or *Hyaloglanis* are unlikely to occur in the northern Guyana Shield versants, except for the Essequibo and the occasional high-order stream capture in headwaters next to those of the Amazonian versant. Species of *Salpynx* are probably not going to be found beyond of any of the major drainages where they are already recorded, except for the Uatumã and adjacent minor basins draining the Amazonian portion of the Guyana Shield. *Hyaloglanis* will probably not be found in the Xingu and Tocantins-Araguaia, major rivers which lie outside of the Central Blackwater Amazon.

AUTHORS´CONTRIBUTIONS: MdP: Conceptualization, Resources, Supervision, Writing – original draft; VR: Formal analysis; CDN: Validation; MdP, VR: Data curation; MdP, VR, CDN: Investigation; VR, CDN: Writing – review & editing. All authors actively participated in the discussion of the results; they reviewed and approved the final version of the paper.

CONFLICT OF INTEREST: Authors declare there are no conflicts of interest.

FUNDING INFORMATION: Funding is provided by CNPq (#315634/2023-5, MdP) and FAPESP (#2020/13433-6 and #2024/22626-3, VR).

ACKNOWLEDGMENTS: We thank Efrem Ferreira for detailed first-hand information on the collection of *Salpynx trombetensis,* which clarified the type locality and habitat. Douglas Bastos provided important ecological information obtained on the occasion of the collection of the type series of *S. ephebus.* Nathan Lujan and Mark Sabaj kindly provided access to CT Scan images and photographs of *Salpynx amapaensis* ANSP 208058 and 209580. Felipe Villegas and Jorge E. García-Melo kindly prepared photographs of, respectively, live and preserved specimens of *Hyaloglanis pulex.* K. Álvarez-Álvarez and M. Hernández helped with the preparation of the map. We are also grateful to Lucia Rapp Py-Daniel for providing INPA database information and access to study material. M. Pastana and M. Romangnolli called our attention to the peculiar pigmentation pattern of live *Microschemobrycon.* The expedition which secured specimens of *S. ephebus,* 'Biodiversity of the Serra da Mocidade', was the result of a collaboration between the Instituto Nacional de Pesquisas da Amazônia (INPA), Instituto Chico Mendes de Conservação da Biodiversidade (ICMBio), Comando Militar da Amazônia (CMA), and Grifa Filmes. Microtomography imaging by A. Carvalho and V. Tambellini (μCT Imaging Laboratory – MZUSP) is gratefully acknowledged. The manuscript greatly benefitted from reviews by J. Ferrer and L. Peixoto, and from conversations with F. Dagosta.

REFERENCES

Arratia, G. & Huaquin, L. 1995. Morphology of the lateral line system and of the skin of diplomystid and certain primitive loricarioid catfishes and systematic and ecological considerations. *Bonner Zoologische Monographien,* 36: 1-110.

Baldwin, C.C. 2013. The phylogenetic significance of colour patterns in marine teleost larvae. *Zoological Journal of the Linnean Society,* 168(3): 496 563. https://doi.org/10.1111/zoj.12033

Baskin, J.N. 1973. *Structure and relationships of the Trichomycteridae.* New York, City University of New York, PHD Faculty of Biology.

Bockmann, F.A. & Sazima, I. 2004. *Trichomycterus maracaya,* a new catfish from the upper rio Paraná, southeastern Brazil (Siluriformes: Trichomycteridae), with notes on the *T. brasiliensis* species-complex. *Neotropical Ichthyology,* 2(2): 61-74. https://doi.org/10.1590/S1679-62252004000200003

Canto, A.L.C.; Hercos A.P. & Ribeiro F.R.V. 2022. Description of a new species of miniature catfish of the genus *Ammoglanis* (Siluriformes: Trichomycteridae) from rio Tapajós basin, Brazil. *Neotropical Ichthyology,* 20(2): 1-13, e210122: 1-13. https://doi.org/10.1590/1982-0224-2021-0122

Chardon, M. 1968. Anatomie comparée de l'appareil de Weber et des structures connexes chez les siluriformes. *Annales du Musée Royal de l'Afrique Centrale,* 169: 1-277.

Costa, W.J.E.M. & Bockmann, F.A. 1994. *Typhlobelus macromycterus,* a new blind glanapterygine fish (Siluriformes, Trichomycteridae) from the Rio Tocantins, Brazil. *Tropical Zoology,* 7: 67-72. https://doi.org/10.1080/03946975.1994.10539241

Costa, W.J.E.M. & Katz, A.M. 2021. Comparative morphology, phylogeny, classification and evolution of interstitial habits in microcambevine catfishes (Siluriformes: Trichomycteridae). *Taxonomy,* 1(4): 313-344. https://doi.org/10.3390/taxonomy1040025

Costa, W.J.E.M.; Henschel, E. & Katz, A.M. 2019a. Multigene phylogeny reveals convergent evolution in small interstitial catfishes from the Amazon and Atlantic forests (Siluriformes: Trichomycteridae). *Zoologica Scripta,* 49: 1-15. https://doi.org/10.1111/zsc.12403

Costa, W.J.E.M.; Mattos, J.L.O. & Santos, A.C.A. 2019b. *Ammoglanis multidentatus,* a new miniature sand-dwelling sarcoglanidine catfish with unique osteological features from northeastern Brazil (Siluriformes: Trichomycteridae). *Vertebrate Zoology,* 70(1): 61-67.

Dagosta, F.C.P. & de Pinna, M. 2019. The fishes of the Amazon: distribution and biogeographical patterns, with a comprehensive list of species. *Bulletin of the American Museum of Natural History,* 431(13): 1-163. https://doi.org/10.1206/0003-0090.431.1.1

DoNascimiento, C. 2015. Morphological evidence for the monophyly of the subfamily of parasitic catfishes Stegophilinae (Siluriformes, Trichomycteridae) and phylogenetic diagnoses of its genera. *Copeia,* 103(4): 933-960. https://doi.org/10.1643/CI-14-132

Ferreira, E.J.G. 1993. Composição, distribuição e aspectos ecológicos da ictiofauna de um trecho do Rio Trombetas, na área de influência da futura UHE Cachoeira Porteira, Estado do Pará, Brasil. *Acta Amazônica,* 23(Supl.): 1 89. https://doi.org/10.1590/1809-43921993235089

Ferrer, J. 2016. *Filogenia e revisão taxonômica do gênero Scleronema (Siluriformes: Trichomycteridae).* Porto Alegre, Universidade Federal do Rio Grande do Sul, 249p. (Tese Doutorado)

Goda, M. & Fujii, R. 1996. Biology of the chromatophores of the ice goby, *Leucopsarion petersii. Zoological Science,* 13(6): 783 793. https://doi.org/10.2108/zsj.13.783

Henschel, E.; Mattos, J.L.O.; Katz, A.M. & Costa, W.J.E.M. 2017. Position of enigmatic miniature trichomycterid catfishes inferred from molecular data (Siluriformes). *Zoologica Scripta,* 57(1): 44-53, 2018. https://doi.org/10.1111/zsc.12260

Henschel, E.; Bragança, P.H.N.; Rangel-Pereira, F. & Costa, W.J.E.M. 2020a. A new psammophilic species of the catfish genus *Ammoglanis* (Siluriformes: Trichomycteridae) from the Amazon River basin, northern Brazil. *Zoosystematics and Evolution,* 96(1): 67-72. https://doi.org/10.3897/zse.96.48952

Henschel, E.; Lujan, N.K. & Baskin, J.N. 2020b. *Ammoglanis natgeorum,* a new miniature pencil catfish (Siluriformes: Trichomycteridae) from the lower Atabapo River, Amazonas, Venezuela. *Journal of Fish Biology,* 97(5): 1481-1490. https://doi.org/10.1111/jfb.14515

Henschel, E.; Ohara, W.M. & Costa, W.J.E.M. 2023. Two new miniature translucent catfish species of the rare genus *Tridens* (Siluriformes: Trichomycteridae) from the Madeira River basin, northern Brazil. *Journal of Fish Biology,* 103(1): 155-171. https://doi.org/10.1111/jfb.15403

Mattos, J.L.O.; Costa W.J.E.M. & Gama C.S. 2008. A new minature species of *Ammoglanis* (Siluriformes: Trichomycteridae) from the Brazilian Amazon. *Ichthyological Exploration of Freshwaters,* 19(2): 161-166.

Nilsson-Sköld, H.N.; Sara-Aspengren, S.; Cheney, K.L. & Margareta, W. 2016. Fish chromatophores – from molecular motors to animal behavior. *International Review of Cell and Molecular Biology,* 321: 171-219. https://doi.org/10.1016/bs.ircmb.2015.09.005

Nilsson-Sköld, H.N.; Svensson, P.A. & Zejlon, C. 2010. The capacity for internal color change is related to body transparency in fishes. *Pigment Cell & Melanoma Research,* 23(2): 292-295. https://doi.org/10.1111/j.1755-148X.2010.00674.x

Ochoa, L.E.; Datovo, A.; DoNascimiento, C.; Roxo, F.F.; Sabaj, M.H.; Chang, J.; Melo, F.B.; Silva, G.C.; Foresti, F.; Alfaro, M. & Oliveira, C. 2020. Phylogenomic analysis of trichomycterid catfishes (Teleostei: Siluriformes) inferred from ultraconserved elements. *Scientific Reports,* 10(1): 1-15. https://doi.org/10.1038/s41598-020-59519-w

Ochoa, L.E.; Roxo, F.F.; DoNascimiento, C.; Sabaj, M.H.; Datovo, A.; Alfaro, M. & Oliveira, C. 2017. Multilocus analysis of the catfish family Trichomycteridae (Teleostei: Ostariophysi: Siluriformes) supporting a monophyletic Trichomycterinae. *Molecular Phylogenetics and Evolution,* 115: 71-81. https://doi.org/10.1016/j.ympev.2017.07.007

Ohara, W.; Jerep, F.C. & Cavallaro, M.R. 2019. A new species of *Microschemobrycon* (Characiformes: Characidae) from Rio Xingu basin, Brazil. *Zootaxa,* 4576(2): 326-336. https://doi.org/10.11646/zootaxa.4576.2.6

Pastana, M.N.L.; Bockmann, F.A. & Datovo, A. 2019. The cephalic lateral-line system of Characiformes (Teleostei: Ostariophysi): anatomy and phylogenetic implications. *Zoological Journal of the Linnean Society,* 189(1): 1-46, 2020. https://doi.org/10.1093/zoolinnean/zlz105

de Pinna, M.C.C. 1988. A new genus of trichomycterid catfish (Siluroidei, Glanapteryginae), with comments on its phylogenetic relationships. *Revue Suisse de Zoologie,* 95: 113-128. https://doi.org/10.5962/bhl.part.79642

de Pinna, M.C.C. 1989. Redescription of *Glanapteryx anguilla,* with notes on the phylogeny of Glanapteryginae (Siluriformes, Trichomycteridae). *Proceedings of the Academy of Natural Sciences of Philadelphia,* 141: 361-374.

de Pinna, M.C.C. 1992. A new subfamily of Trichomycteridae (Teleostei, Siluriformes), lower loricarioid relationships and a discussion on the impact of additional taxa for phylogenetic analysis. *Zoological Journal of the Linnean Society,* 106: 175-229. https://doi.org/10.1111/j.1096-3642.1992.tb01247.x

de Pinna, M.C.C., 1998. Phylogenetic relationships of Neotropical Siluriformes: historical overview and synthesis of hypotheses. *In:* Malabarba, L.R.; Reis, R.E.; Vari, R.P.; Lucena, Z.M.S. & Lucena, C.A.S. (Eds.). *Phylogeny and classification of Neotropical fishes.* Porto Alegre, EDIPUCRS. p. 279-330.

de Pinna, M.C.C. 2016. The dawn of phylogenetic research on Neotropical fishes: a commentary and introduction to Baskin (1973), with an overview of past progress on trichomycterid phylogenetics. *Neotropical Ichthyology,* 14(2): 1-11, e150127. https://doi.org/10.1590/1982-0224-20150127

de Pinna, M.C.C. & Dagosta, F.C.P. 2022. A taxonomic review of the vampire catfish genus *Paracanthopoma* Giltay, 1935 (Siluriformes, Trichomycteridae), with descriptions of nine new species and a revised diagnosis of the genus. *Papéis Avulsos de Zoologia,* 62(72): 1-90, e202262072. https://doi.org/10.11606/1807-0205/2022.62.072

de Pinna, M.C.C. & Kirovsky, A.L. 2011. A new species of sand-dwelling catfish, with a phylogenetic diagnosis of *Pygidianops* Myers (Siluriformes, Trichomycteridae, Glanapteryginae). *Neotropical Ichthyology,* 9(3): 493-504. https://doi.org/10.1590/S1679-62252011000300004

de Pinna, M.C.C. & Starnes, W. 1990. A new genus and species of Sarcoglanidinae from the Rio Mamoré, Amazon Basin, with comments on subfamilial phylogeny (Teleostei, Trichomycteridae). *Journal of the Zoological Society,* 222: 75-88. https://doi.org/10.1111/j.1469-7998.1990.tb04030.x

de Pinna, M.C.C. & Winemiller, K.O. 2000. A new species of *Ammoglanis* (Siluriformes: Trichomycteridae) from Venezuela. *Ichthyological Exploration of Freshwaters,* 11(3): 255-264.

de Pinna, M.C.C.; Peixoto, L.; Tagliacollo, V. & Britto, M. In press. Phylogenetic relationships and evolution of the major groups of Siluriformes. *In:* Arratia, G. & Reis, R. (Eds.). *Catfishes, a highly diversified group, evolution and phylogeny.* London, CRC Press. v. 2

de Pinna, M.C.C; Reis, V.J.C.R.; Pastana, M.N.L. & Datovo, A. 2024. A new species of the tridentine *Rhinotridens* from the Amazon basin (Siluriformes: Trichomycteridae). *Neotropical Ichthyology,* 22(2): 1-22. https://doi.org/10.1590/1982-0224-2024-0025

Reis, N.J.; Cordani, U.G.; Goulart, L.E.A.; Almeida, M.E.; Oliveira, V.; Maurer, V.C. & Wahnfried, I. 2021. Zircons U-Pb SHRIMP ages of the Demeni-Mocidade Domain, Roraima, Southern Guiana Shield: extension of the Uatumã Silicic Large Igneous Province. *Journal of Geological Survey of Brazil,* 4(1): 61-78. https://doi.org/10.29396/jgsb.2021.v4.n1.4

Reis, V.J.C. 2023. *Ontogeny and phylogeny in Trichomycteridae (Teleostei, Siluriformes): patterns in the development of morphological complexes.* São Paulo, Ph.D. Dissertation of University of São Paulo. Brazil.

Reis, V.J.C.; de Pinna, M.C.C. & Pessali, T.C. 2019. A new species of *Trichomycterus* Valenciennes 1832 (Trichomycteridae: Siluriformes) from the Rio Doce drainage with remarkable similarities with Bullockia and a CT-scan survey. *Journal of Fish Biology,* 95(3): 918-931. https://doi.org/10.1111/jfb.14089

Reis, V.J.C.; Lecointre, G. & de Pinna, M.C.C. *In press.* The Trichomycteridae: An overview of the systematics and classification of the family. *In:* Arratia, G. & Reis, R. (Eds.). The Catfishes.

Rivera-Rivera, C.J.R. & Montoya-Burgos, J.I. 2018. Back to the roots: Reducing evolutionary rate heterogeneity among sequences gives support for the early morphological hypothesis of the root of Siluriformes (Teleostei: Ostariophysi). *Molecular Phylogenetics and Evolution,* 127: 272-279. https://doi.org/10.1016/j.ympev.2018.06.004

Rizzato, P.P. & Bichuette, M.E. 2016. The laterosensory canal system in epigean and subterranean *Ituglanis* (Siluriformes: Trichomycteridae), with comments about troglomorphism and the phylogeny of the genus. *Journal of Morphology,* 278: 4-28. https://doi.org/10.1002/jmor.20616

Taylor, W.R. & van Dyke, G.C. 1985. Revised procedures for staining and clearing small fishes and other vertebrates for bone and cartilage study. *Cybium,* 9(2): 107-109.

Weitzman, S.H. 1974. Osteology and evolutionary relationships of the Sternoptychidae, with a new classification of stomiatoid families. *Bulletin of the American Museum of Natural History,* 153(3): 327-478.

Wosiacki, W.B.; Coutinho, D.P. & de Assis Montag, L.F. 2011. Description of a new species of sand-dwelling catfish of the genus *Stenolicmus* (Siluriformes: Trichomycteridae). *Zootaxa,* 2752: 62-68. https://doi.org/10.11646/zootaxa.2752.1.3

Zuanon, J. & Sazima, I. 2004. Natural history of *Stauroglanis goudingi* (Siluriformes: Trichomycteridae), a miniature sand-dwelling candiru from Central Amazonian streamlets. *Ichthyological Exploration of Freshwaters,* 14(3): 201-208.

Published with the financial support of the "Programa de Apoio às Publicações Científicas Periódicas da Universidade de São Paulo"